

Final
SUM 97

Piezoelectric Power Consumption for
Active Vibration Control

By

Matthew Charles Brennan

Mechanical Engineering(B.S.) 5/95, The University of Vermont

A Thesis submitted to

The Faculty of

The School of Engineering and Applied Science,
of The George Washington University in partial satisfaction
of the requirements for the degree of Master of Science

July 25, 1997

Thesis directed by

Dr. Robert H. Tolson

Professor of Engineering and Applied Science

This research was conducted at NASA Langley Research Center.

ABSTRACT

A method for predicting the power consumption of piezoelectric actuators utilized for active vibration control is presented. Analytical developments and experimental tests show that the maximum power required to control a structure using surface-bonded piezoelectric actuators can be estimated without modeling the dynamics between the piezoelectric actuator and the host structure. The results demonstrate that for a perfectly-controlled structure, the power consumption of the piezoelectric actuator is a function of the effective capacitance of the actuator and the voltage and frequency of the control law output signal. Furthermore, as control effectiveness decreases, the power consumption of the piezoelectric actuator decreases. For typical surface-bonded piezoelectric actuators, the power required for active vibration control can be conservatively determined within 90% accuracy without modeling the structural dynamics of the actuator and host structure. Also, a non-linear behavior in the capacitance of piezoelectric actuators was identified. This research revealed a 0.44% increase in capacitance per volt, or an 88% increase in capacitance at the maximum operating voltage of the actuator. A method is presented to account for the non-linearity. Also, problems and associated solutions that are encountered with using piezoelectric actuators for control are discussed.

ACKNOWLEDGEMENTS

This work was supported by NASA Grant NCC1-208. I would like to extend special thanks to Anna McGowan for giving me drive and motivation in my research and for all the extra support that went beyond her responsibilities as my advisor to make my career as memorable, enjoyable and successful as it has become. Thanks to Carol Weisman and Jennifer Heeg for their help and support throughout my research. Also, Thanks to everyone in the Aeroelasticity Branch at NASA Langley that made my time there more enjoyable. I also extend my appreciation to Robert Tolson for giving me this opportunity to take part in the JIAFS program and to Tom Noll and Boyd Perry for allowing me to conduct my research at the Aeroelasticity Branch. Finally, I want to thank Steve for being there through the good and bad and helping me maintain some sanity over the past two years.

TABLE OF CONTENTS

ABSTRACT	ii
ACKNOWLEDGEMENTS	iii
TABLE OF CONTENTS	iv
VARIABLES AND NOMENCLATURE	vi
LIST OF FIGURES	ix
CHAPTER 1: INTRODUCTION	1
1.0 Motivation	1
1.1 Piezoelectric Actuators	2
1.2 Active Control with Piezoelectric Actuators	4
1.3 Power Amplifiers	7
1.4 Objective	9
1.5 Outline	10
CHAPTER 2: LITERATURE REVIEW	12
2.0 Introduction to Literature Review	12
2.1 Electro-Mechanical Impedance Model	12
2.2 Rayleigh-Ritz Approximation	13
2.3 Summary	14
CHAPTER 3: ANALYTICAL DEVELOPMENT OF POWER	16
3.0 Introduction to Analysis	16
3.1 Solutions of Piezoelectric Constitutive Equations	19

3.1a Stress-Strain Relationship	20
3.1b Solutions For Current	21
3.2 Actuator Strain	23
3.2a Structural Equation of Motion	25
3.2b Equation of Motion and Actuator Strain	26
3.3 Structural Control	28
3.3a Perfect Control	29
3.3b Imperfect Control	30
3.3c Boundaries on Admittance	32
3.4 Piezoelectric Power Required for Active Control	35
CHAPTER 4: RESULTS	38
4.0 Introduction to Results	38
4.1 Single-Degree-Of-Freedom Test Structure	39
4.2 Non-Linear Capacitance	41
4.3 Open-Loop Excitation	45
4.4 Feed-Forward Control(constant amplitude excitation)	47
4.5 Closed-Loop Control(strain-feedback)	53
CHAPTER 5: CONCLUSION	57
APPENDIX 1: Electrical Analysis	59
APPENDIX 2: Non-Linear Capacitance Plots	65
APPENDIX 3: ACX Actuator Material Properties and Geometry	66
REFERENCES	69

VARIABLES AND NOMENCLATURE

C = Effective capacitance

c = Damping of host structure

D_3 = Electric displacement

d_{31} = Piezoelectric constant

E = Electric field

F_e = External force

F_a = Piezoelectric actuator force

G, g = Generic variable

h = Actuator thickness

I, i = Current

k = Stiffness of host structure

k_a = Effective stiffness of piezoelectric actuator

L = Actuator length

m = Mass of the host structure

P = Power

Q = Charge

S_1 = Strain of piezoelectric actuator

s = Complex variable

T_1 = Stress acting on piezoelectric actuator

t = Time

V = Voltage

w = Actuator width

x = x-direction, displacement in x-direction

Y = Electrical admittance

Y_{11} = Piezoelectric elastic modulus

y = y-direction

z = z-direction

ϵ_{33} = Dielectric constant

ϕ = Phase angle

ω_n = Natural frequency

ω = Radial frequency

ζ = Damping coefficient

$\frac{\partial g}{\partial t}$ = Derivative of g with respect to t

$\text{Re}[G]$ = The real component of G

$\text{Im}[G]$ = Imaginary component of G

$|G(\omega)|$ = The magnitude of G

$G^*(\omega)$ = Complex conjugate of G

$\mathcal{L}[g(t)]$ = Laplace Transform of $g(t)$

EOM = Equation of motion

SDOF = Single-degree-of-freedom

MDOF = Multiple-degree-of-freedom

PARTI = Piezoelastic Aeroelastic Response Tailoring Investigation

ACROBAT = Actively Controlled Response Of Buffet Affected Tails

LIST OF FIGURES

Figure 1.1: Illustration of Piezoelectric Effect. Element excited in thickness with displacement in extension	2
Figure 1.2: Illustration of PZT Actuator Types(note: orientation of axis change).	4
Figure 1.3: Diagram of Moments Generated by Piezoelectric Actuator.	4
Figure 1.4 : General Diagram of Controller-Amplifier-Structure Setup.	5
Figure 1.5: Illustration of Internal Structure of PARTI Wing	6
Figure 1.6: PARTI Wing With Aerodynamic Shells.	6
Figure 1.7: Photograph of Internal Structure of PARTI Wing.	6
Figure 1.8: F-18 Wind-Tunnel Test Model With PZT Actuators Embedded In Vertical Tail.	7
Figure 1.9: Vertical Tail Embedded With PZT Actuators.	7
Figure 3.1: Diagram of Components in Piezoelectric Admittance	18
Figure 3.2: Illustration of Piezoelectric actuator orientation	19
Figure 3.3: Figure 3.3: Simplification of Cantilever Beam to SDOF Structure.	25
Figure 3.4: Diagram of Actuator and External Force.	31
Figure 3.5: Strain and Voltage Relationship for Active Control	33
Figure 4.1: Picture Of Single-Degree-of-Freedom Test Structure	39
Figure 4.2: Illustration Of Test Setup	40
Figure 4.3: Capacitance vs. Excitation Voltage for the Actual, Analytical and the Empirical Model of Capacitance	42
Figure 4.4: Open-Loop Excitation Response of Admittance and Strain to Voltage Response. Both Plots Have Been Normalized by Max Values.	46
Figure 4.5: Diagram of Open-Loop Control Law.	49

Figure 4.6 A(top) and B(bottom): The PSD of Strain for Test A and Test B With Piezoelectric Actuator On and Off.	50
Figure 4.7: Relative Admittance Between Empirical model, Test A and Test B.	51
Figure 4.8: Percent Error Between the Empirical Model And Tests A and B.	52
Figure 4.9: Diagram of Closed-Loop Control Law.	53
Figure 4.10: Frequency Response of Calculated Maximum Admittance and Actual Admittance.	54
Figure 4.11: Frequency Response of Estimated Admittance and Actual Admittance	55
Figure 4.12: Plots of Actual Power and Estimated Power vs. Frequency.	56

CHAPTER 1: INTRODUCTION

1.0 Motivation

In recent years, a new category of engineering optimization has evolved referred to as "smart structures". Smart structures are a step in engineering evolution from the traditional "static" structures to more active "kinetic" structures. Smart structures transgress from the optimization of static structures with material and structural efficiency to the passive or active control of the structure's state (displacement and rate) and properties (stiffness and damping) by utilizing a kinetic ability through extensive actuator, sensor and processor arrays. This will allow smart structures to adapt to changing boundary conditions, expanding the capacity and efficiency of the structures under a variety of conditions. (1)

Smart structures have been researched in many aspects of engineering including applications in medical technology, civil structures and aerospace. The materials found to be most successful are shape memory alloys and piezoelectric materials (1,2). Shape memory alloys (SMA's) are characterized by the ability to return to a pre-stressed shape with applied heat. SMA's typically have a bandwidth on the order of one hertz or less and are suitable for shape control and passive vibration control. For instance, Lockheed Martin is investigating the feasibility of using SMA's to actively control the twist of an aircraft wing to increase the flight envelope of the aircraft (3). The second group of smart materials are piezoelectric materials. Piezoelectric actuators induce a strain or force when exposed to an electric field. With a bandwidth on the order of several kilohertz, piezoelectric actuators are more suitable for acoustics and vibration control.

The current research is an investigation of the power requirements of piezoelectric actuators during active vibration control. Whether piezoelectric actuators require an excessive quantity of electrical power is a concern in assessing the feasibility of piezoelectric actuators utilized for active control. First, a brief introduction of piezoelectric materials will be discussed. Then the types of piezoelectric actuators and how they are applied will be introduced. Also, previous research that demonstrates the capability of piezoelectric actuators will be presented. Next, an overview of past efforts in identifying piezoelectric power characteristics will precede the analysis and an experimental verification will conclude the paper.

1.1 Piezoelectric Actuators

The piezoelectric effect is the capacity of the material to change in dimension when exposed to an electric field or generate a charge when exposed to a stress or strain. The ability to couple electrical energy with mechanical energy is the unique behavior that make piezoelectric materials ideal for actuation and sensing (Figure 1.1).

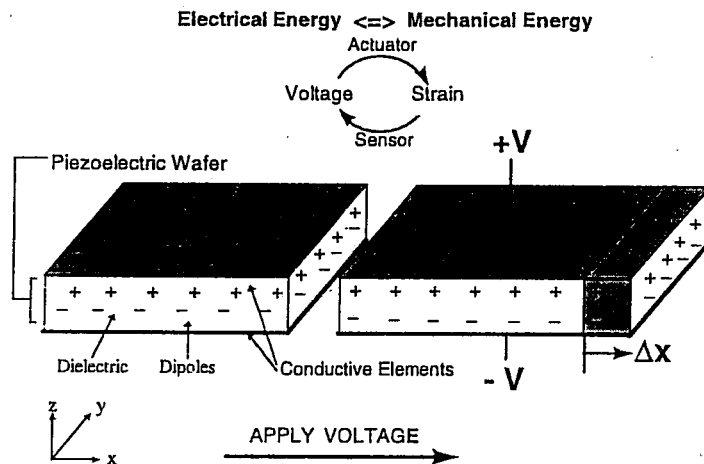


Figure 1.1: Illustration of Piezoelectric Effect. Element Excited in Thickness With Displacement in Extension

Piezoelectric material is made up of two distinct parts that allow for the piezoelectric effect: a dielectric material and electric dipoles. The dielectric material is any non-conductive material, such as the material found in a capacitor, and makes up most of the piezoelectric material. The electric dipoles are found throughout the dielectric material. Electric dipoles are any molecule, element or ion that contains an opposite charge on opposite ends, also referred to as polar charges. In the piezoelectric material, the dipoles are aligned so that the electric force created by the polar charge can be utilized to generate a force. By applying an electric field to the material, the dipoles are attracted to the electric field, inducing a force or strain in the piezoelectric material (Figure 1.1). An electric potential is generated when the piezoelectric material is strained due to the dipoles which are forced to shift.

Most piezoelectric actuators are composed of PbZrO_3 (PZT) type piezoelectric material. These actuators are commonly applied in two physical orientations, stack and laminar actuators (Figure 1.2). PZT stack actuators utilize displacements in the thickness. PZT surface-bonded laminar actuators utilize the displacement along its length when excited through the thickness. Despite what the name of each actuator type implies, both actuator types will displace in all 3 axis when excited through the thickness. The dominant change in dimension is typically identified by the dominant magnitude in geometry. For example, stack actuators predominant magnitude in geometry is the thickness. Surface-bonded laminar actuators predominant magnitude in geometry is the length. PZT surface-bonded laminar actuators will be the topic of analysis in this paper.

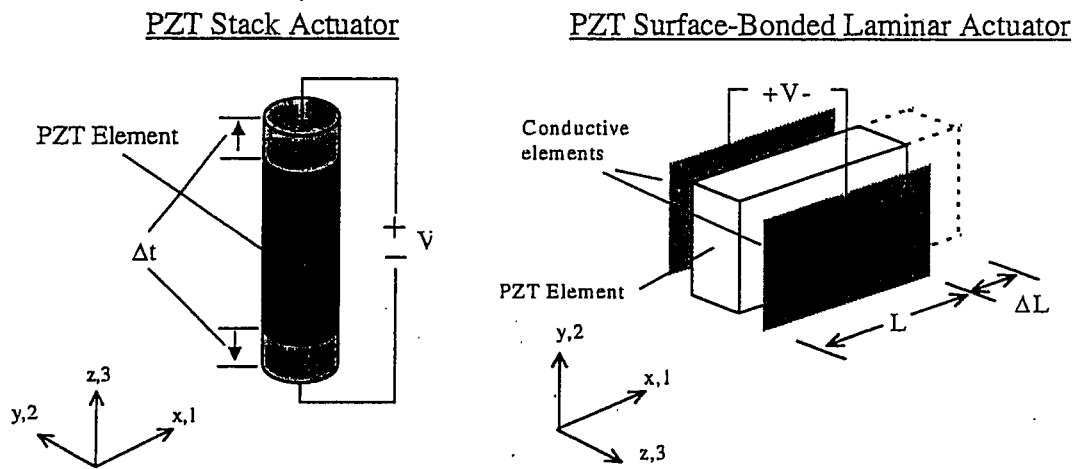


Figure 1.2: Illustration of PZT Actuator Types (note: orientation of axis change)

1.2 Active Control with Piezoelectric Actuators

Using surface-bonded laminar actuators, a net moment can be induced on a plate or beam-like structure by adhering the piezoelectric actuators to the top and bottom face of the plate. By exciting the two actuators 180 degrees out of phase, a net moment is generated about the neutral axis of the beam or plate (Figure 1.3).

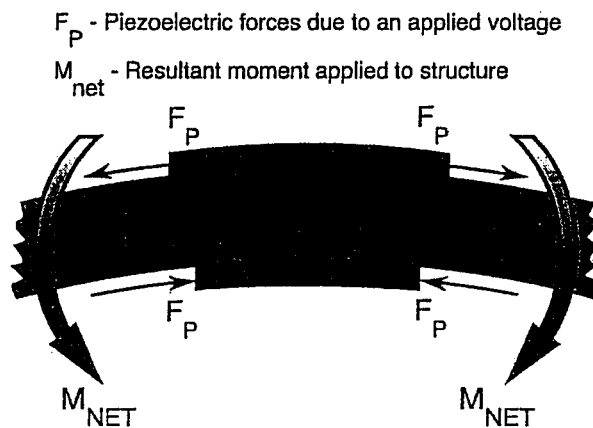


Figure 1.3: Diagram of Moments Generated By Piezoelectric Actuator

A diagram of the general test setup during active vibration control is shown in Figure 1.4.

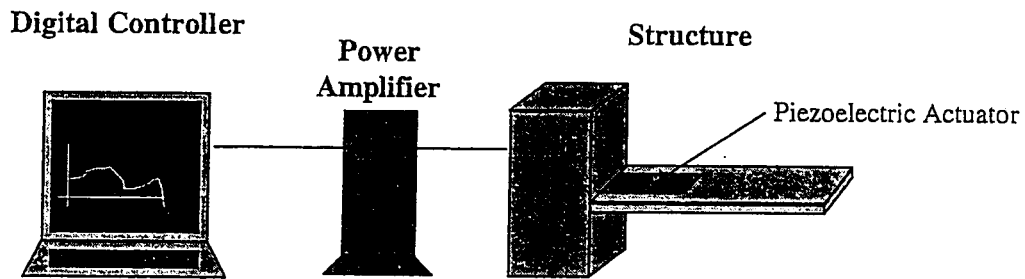


Figure 1.4 : General Diagram of Controller-Amplifier-Structure Setup.

The benefits found in using piezoelectric actuators for active control have been displayed in numerous ground tests and wind-tunnel demonstrations (4-16). The current research was motivated by the Piezoelectric Aeroelastic Response Tailoring Investigation (PARTI) (4,5). During this study, a four foot long semi-span wing model with 72 distributed piezoelectric actuators was used to demonstrate that piezoelectric actuation can effectively control aeroelastic response. Illustrations and photographs of the PARTI wing are supplied by NASA Langley Research Center (Figures 1.5, 1.6 and 1.7).

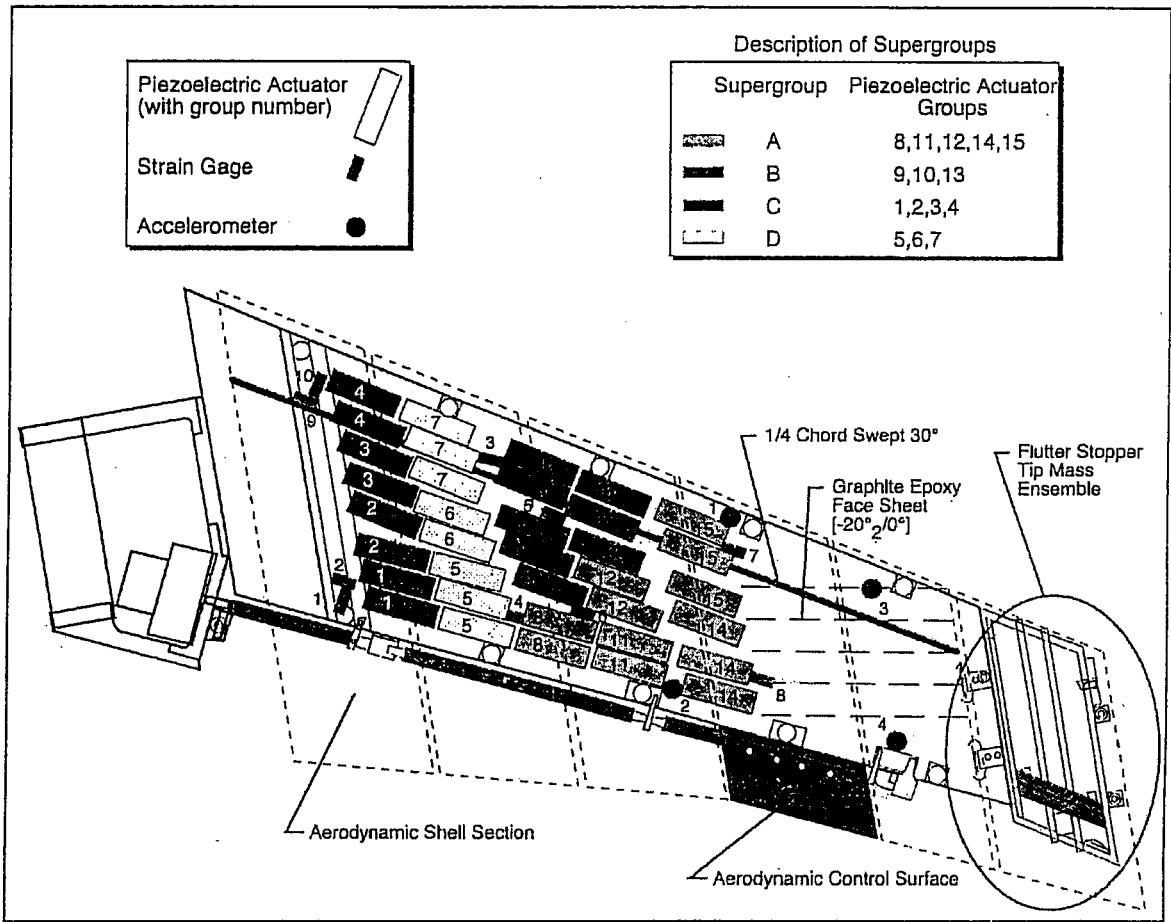


Figure 1.5: Illustration of Internal Structure of PARTI Wing

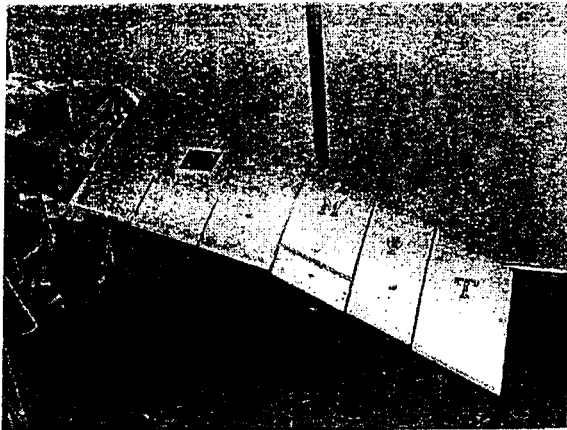


Figure 1.6: PARTI Wing With Aerodynamic Shells.

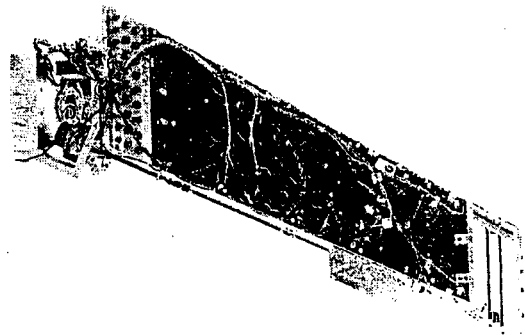


Figure 1.7: Photograph of Internal Structure of PARTI Wing.

A more recent program is the ACROBAT program (6) where piezoelectric actuators were successfully used to reduce damaging vibration in the vertical stabilizers of an F-18 wind-tunnel test model. Illustrations and photographs of ACROBAT test model are supplied by NASA Langley Research Center (Figures 1.8 and 1.9). Presently, a full scale F-18 aircraft is being fitted with piezoelectric actuators to demonstrate that the actuators are effective on full-scale aircraft.



Figure 1.8: F-18 Wind-Tunnel Test Model With PZT Actuators Embedded In Vertical Tail.

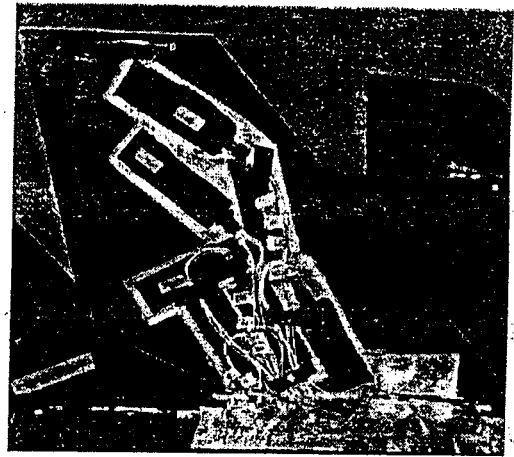


Figure 1.9: Vertical Tail Embedded With PZT Actuators.

1.3 Power Amplifiers

The following analysis and verification will determine the power requirements of a piezoelectric actuator used for active vibration control. Although this is the power required by the actuator, this is not necessarily the "wall power" required to power the actuators. Wall power refers to the amount of power required by the power amplifiers to power the actuators, or the power running through the plug of the power amplifier. The analysis will show that the admittance of the actuator is primarily due to a capacitance

load. Capacitors require a reactive power, identified by the 90 degree phase lag between the current and voltage. A description of reactive power is given in Appendix 1.

Different amplifiers power the reactive load in different ways, the result is a drastic difference in the efficiency of power amplifiers. Efficiency of the amplifier refers to the amount of power generated relative to the amount of power required to generate a signal.

There are currently three types of power amplifiers available for piezoelectric actuation: linear amplifier, switching amplifier (Piezo Systems, Inc.) and switching capacitor amplifier (Lucent Technologies, 28). Linear amplifiers are the more traditional amplifiers used in most piezoelectric applications. Due to the reactive load of the piezoelectric actuators noted above, a new generation of power amplifiers have been developed, tailored to power the reactive load: switching amplifiers and switching capacitor amplifiers.

Linear amplifiers are the least efficient because of the method used to amplify the reactive signal. The linear amplifier charges the capacitor, or piezoelectric material, with the entire power output. On the discharge, all the stored charge in the capacitor is dumped to ground. This is the mechanical equivalent of compressing a mass-spring system, taking the mass off the spring to let the spring expand, and lifting the mass onto the spring again only to repeat the process. The result is a tremendous loss in potential energy.

Switching amplifiers and switching capacitor amplifiers are designed to store the potential energy so that the energy can be used again to recharge the capacitor. By doing this, the potential energy in the capacitor is maintained and the overall power consumption is drastically reduced. The switching amplifier and switching capacitor

amplifier use different mechanisms to perform this task. Details of these mechanism are not available at this time because the amplifiers are a new technology and detailed information on the amplifiers is not yet available. For the same reason, the effectiveness of these amplifiers in the control of piezoelectric actuators is also unknown. Linear amplifiers demonstrate good control behavior including large bandwidth, low noise, constant gain and negligible phase loss and are still the amplifiers of choice at this time.

In summary, the equation of power developed in the Analysis Section applies to the linear amplifier. For the new generation of switching amplifiers and switching capacitor amplifiers, the reactive power requirements of the piezoelectric actuator would become negligible and the overall power loss would be due to losses in the electrical system. The electrical system refers to the power amplifier and the piezoelectric actuator. Thus, knowing the type of power amplifier being used is crucial to determining the total power consumption of piezoelectric actuators.

1.4 Objective

One critical issue raised by these studies is whether full-scale airplanes and other large structures will require excessive power to use piezoelectric actuators for active vibration control. Piezoelectric materials are complex to model as actuators due to the piezoelectric effect that defines the electro-mechanical coupling within the actuator. The piezoelectric power characteristics become a function of the material properties of the piezoelectric actuator as well as the mechanical dynamics between the actuator and the host structure. Modeling the dynamics between the piezoelectric actuator and the host structure has proven to be an extremely complex task to complete for structures as large

or larger than the PARTI wing (17,18). Thus, piezoelectric power characterization of actuators controlling complex structures may be extremely complex to determine.

For simple plate and beam models with a few piezoelectric actuators, the actuator and host dynamics are reasonable to solve. Realistically, the host structure will be much more complex than a simple beam or plate and will require complex finite element analysis to develop an estimate of the actuator and host structure dynamics.

The objective of the current research is to more closely define the individual contributions of the material properties and mechanical dynamics on the power characteristics of the piezoelectric actuators during the specific case of active vibration control. The goal is to determine the overall necessity of modeling the complex electro-mechanical relationship between the actuator and the host structure.

1.5 Outline

The following literature review will introduce the two founding techniques available for characterizing piezoelectric power consumption. Liang et. al. (19-22) and Hagood et. al. (23) developed the techniques used by most researchers investigating piezoelectric power consumption. Both techniques are shown to be highly accurate using two distinctly different approaches. The positive and negative attributes of each will be discussed. A third technical reference is from Warkentin (24), who used the techniques presented by Hagood et. al and applied them to closed-loop control.

All three research efforts required an accurate model of the dynamics of the actuator and host structure. The analytical section of this paper extends Warkentin's model and proves

that the influence of the actuator and host structural dynamics are negligible in characterizing piezoelectric power consumption for the specific case of active vibration control.

The experimental section will cover in detail the verification of the analytical model presented. A single-degree-of-freedom cantilevered beam is used with a strain feedback control law. In addition, several related topics will be discussed that include non-linear material properties and power amplifiers for piezoelectric actuator use.

CHAPTER 2: LITERATURE REVIEW

2.0 Introduction to Literature Review

Although piezoelectric actuators have been investigated extensively for active control, research on piezoelectric power consumption is limited to essentially two groups of researchers; Liang et. al. (19-22) and Hagood et. al. (23). The pros and cons of each technique will be discussed.

2.1 Electro-Mechanical Impedance Model

Liang et. al. (19-22) developed a piezoelectric electro-mechanical impedance model.

This electro-mechanical impedance model was derived from the equation of motion of the piezoelectric actuator which was modeled as a plate in longitudinal excitation. The boundary conditions were prescribed by the piezoelectric constitutive equations and coupled with the mechanical impedance of the host structure. Mechanical impedance refers to the ratio of force input to structural velocity, or the ratio of input to response. Thus, the dynamics between the actuator and host structure are directly coupled. The solution includes a coupling between the electro-mechanics of the piezoelectric actuator and the mechanics of the host structure through the impedance of the actuator and host structure. Liang's electro-mechanical impedance model was then applied to determine the power characteristics.

Liang's model only investigated the case of open-loop excitation. Open-loop excitation refers to the case when the piezoelectric actuator is used to excite motion in the structure without feedback. The major benefits of Liang's model are the explicit solutions that allow the investigation of the electrical and mechanical energy exchange between actuator

and host structure. Also, by modeling the equation of motion of the actuator, Liang was able to define the region where the actuator behaves linearly and the region where the actuator's mechanical dynamics affect the control authority of the actuator. Liang's model is an accurate model of piezoelectric actuators, but it is difficult with implement to complex structures. Also, the solution is based on open-loop excitation. Applying closed-loop control or active vibration control proves to be extremely complex.

2.2 Rayleigh-Ritz Approximation

An alternative method is based on the development by Hagood et. al.. Their approach determined the equation of motion of the host structure excited by the piezoelectric actuator. Using a Rayleigh-Ritz approximation to couple the beam with the piezoelectric actuator bonded to it, the strain of the actuator can be determined. Incorporating the strain of the actuator, the piezoelectric constitutive equations are used to determine the power characteristics. The difference between the two methods is that Liang solved for the explicit equation of motion of the actuator bonded to a host structure where Hagood determined the equation of motion of the host structure excited by the piezoelectric actuator while ignoring the mass characteristics of the piezoelectric actuator. Although Hagood's model is not as accurate in modeling the piezoelectric actuator, the model sufficiently couples the dynamics between the actuator and the host structure for most cases. Also, this model can be readily applied to complex structures and closed-loop control.

A comprehensive study was presented by Warkentin of MIT. Warkentin presented a development of piezoelectric power consumption for active vibration control using the

analytical models developed by Hagood et. al.. Warkentin's model directly addresses the characterization of power for piezoelectric actuators during active vibration control.

2.3 Summary

Subsequent research concerning the power consumption of piezoelectric actuators is primarily founded on the two previous methods (14,15,16,24). The conclusion of all previous research for both the excitation of a structure and the closed-loop control of a structure is that the electrical power of piezoelectric actuators is a function of the mechanical motion of the structure and the electrical characteristics of the piezoelectric material. Modeling the mechanical motion is the limiting factor in applying these techniques for active vibration control. As structures controlled by piezoelectric actuators become more complex, modeling the mechanical motion of the actuator and host structure becomes extremely complex.

The current research takes Warkentin's results a step further. An analytical model is developed that shows the influence of the mechanical motion of the host structure are negligible on the power characteristics of the piezoelectric actuator used for active vibration control. When completely controlled, the structure is motionless, thus the power requirements of the piezoelectric actuator are no longer a function of the mechanical motion of the structure. In this ideal scenario, the power is only dependent on geometry and material properties of the piezoelectric actuators and the voltage and frequency of the control law signal. Furthermore, the current research finds that as control effectiveness decreases, the power requirements of piezoelectric actuators

decrease. Thus, the results from this ideal scenario provide an upper bound for the power required.

CHAPTER 3: ANALYSIS

3.0 Introduction to Analysis

The analysis is composed of the derivation of piezoelectric power consumption for the specific case of active vibration control. Appendix 1 defines important electrical quantities and tools required for developing the analysis. For an electrical system with frequency content, the most straightforward way to characterize power requirements is to define the electrical admittance of the circuit.

$$Y(\omega) = \frac{I(\omega)}{V(\omega)} \quad 3.1$$

The electrical admittance, $Y(\omega)$, defines the linear relationship between current, $I(\omega)$ and voltage, $V(\omega)$, in the frequency domain. Frequency is designated by ω . Admittance is related to power; $P(\omega)$, through the equation:

$$P(\omega) = Y(\omega)V^2(\omega) \quad 3.2$$

The analysis will focus on the development of the admittance which can then be applied to the equation of power. The admittance is determined in Section 3.1 from the piezoelectric constitutive equations. Because piezoelectric actuators are electro-mechanical devices, the admittance of piezoelectric actuators is made up of an electrical component and an electro-mechanical component as shown by this generic equation of admittance for piezoelectric materials.

$$Y(\omega) = (\textit{electrical} + \textit{electro-mechanical})$$

The electro-mechanical component couples the motion of the actuator with the electrical characteristics. For an actuator bonded to a structure, the motion of the structure will be coupled with the electrical characteristics of the actuator as well. In fact, the admittance can be broken into the two physical applications that piezoelectric materials are used for, actuator and sensor:

$$Y(\omega) = (\text{actuator} + \text{sensor})$$

Here, the electrical component is identified as the actuator and the electro-mechanical component is identified as the sensor. The solution for the electrical, or actuator, component is developed directly from the constitutive equations of motion shown in Section 3.1. The electro-mechanical, or sensor, component will be the predominant focus of the analysis. The electro-mechanical component will prove to be application specific. For each application, a model of the piezoelectric actuator and host dynamics is necessary, Figure 3.1. For the current research, the specific case of active vibration control is investigated where the model of piezoelectric actuator and host structure dynamics predicts the response of the structure due to a random load and the response of the structure due to the piezoelectric actuators being excited by a specific control law. Due to the vast array of vibration control applications available, the development of a generic solution that is applicable to all active vibration control systems is difficult to achieve.

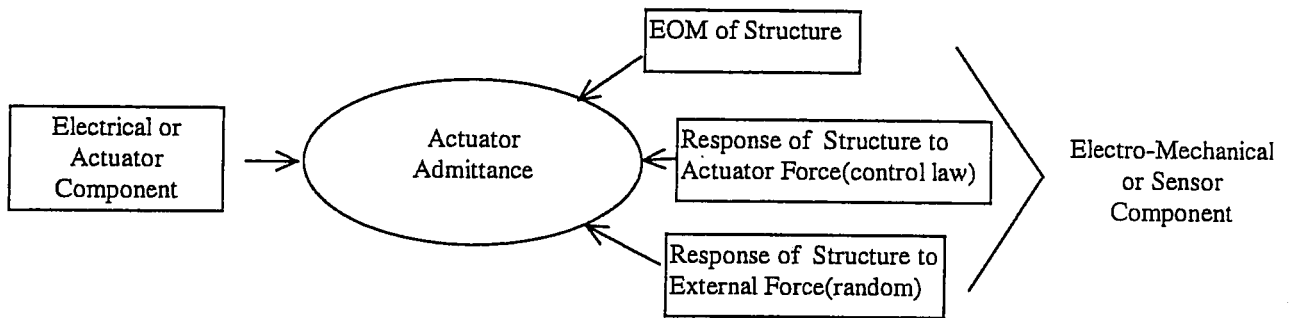


Figure 3.1: Diagram of Components in Piezoelectric Admittance.

After thorough analysis and experimental testing, the sensor component is found to have negligible influence on the overall admittance during active vibration control. The conclusion of the analysis is that an accurate prediction of the admittance, and hence power, can be determined without modeling the effects of the sensor component in the piezoelectric admittance leaving just the actuator component to solve for. As will be seen in the analysis, the actuator component is only made up of material constants and geometry which drastically simplifies the solution of the piezoelectric admittance for active vibration control.

The analysis begins in Section 3.1 with the development of the basic piezoelectric equations from the piezoelectric constitutive equations, including force, strain and admittance. Section 3.2 develops the equation of motion of the actuator bonded to a simple structure. The equation of motion is then applied in Section 3.3 to investigate the case of active vibration control. Section 3.3 is broken into 3 sections. The first section investigates the case of perfect control, where structural motion is completely suppressed. The second section investigates the more realistic case of imperfect control, where motion is not completely suppressed. The third section investigates the best and worst case scenarios for structural control which are then applied to the equation of admittance to

determine when admittance is maximum for active control. The analysis concludes with the equation of power for piezoelectric actuators used for active vibration control.

3.1 Solutions of Piezoelectric Constitutive Equations:

The constitutive equations for a piezoelectric actuator (19) excited in the z-direction and displaced in the x-direction are (orientation of actuator is illustrated in Figure 3.2):

$$S_1 = \frac{1}{Y_{11}} T_1 + d_{31} E$$

or

3.3

$$D_3 = \epsilon_{33} E + d_{31} T_1$$
3.4

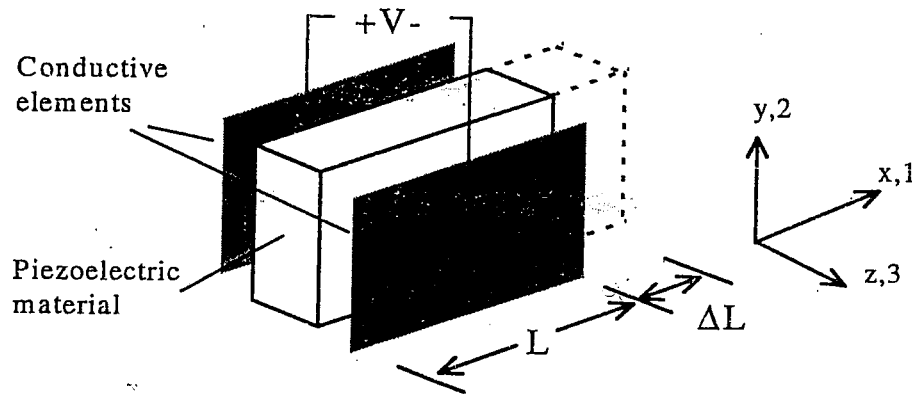


Figure 3.2: Illustration of Piezoelectric actuator orientation

As noted earlier, this paper is investigating surface-bonded laminar actuators; therefore, displacement in the z-axis and y-axis are considered negligible and will not be considered for this derivation. Dielectric and piezoelectric losses are also considered negligible. The electric field, E , is defined as voltage divided by the piezoelectric material thickness: $E =$

Wh. The strain in the actuator is designated by S_1 (or $\frac{\Delta L}{L}$). The stress, T_1 , acting on the actuator can be determined from equation 3.3.

$$T_1 = Y_{11}(S_1 - d_{31}E) \quad 3.5$$

D_3 designates the electric displacement which is defined as the charge per unit area. The charge is determined by integrating the electric displacement over the surface area of the piezoelectric actuator.

$$Q = \iint_{xy} D_3 dx dy \quad 3.6$$

The current is determined by the time derivative of the charge.

$$i(t) = \frac{dQ}{dt} \quad 3.7$$

Several relationships can be defined from these equations:

3.1a Stress-Strain Relationship

From equation 3.5, the relationship between stress and strain is developed. The **blocking force** of the piezoelectric actuator is defined as the force output of the piezoelectric actuator at zero strain.

$$F_{blocking} = -T_1(S_1 = 0) \times Area = d_{31}Y_{11}Ewh = wd_{31}Y_{11}V \quad 3.8$$

The **stroke** of the actuator is determined by setting the stress to zero.

$$S_1(T_1 = 0) = d_{31}E \quad 3.9$$

For a short-circuited piezoelectric actuator (when both electrical poles are grounded or $V = 0$) the stress-strain relationship is defined by Hooke's Law.

$$T_1 = Y_{11}S_1 \quad 3.10$$

3.1b Solutions For Current

From equations 3.4, 3.6 and 3.7, the charge and the current are developed:

$$Q = \iint_{xy} D_3 dx dy = wL[\epsilon_{33}E + d_{31}T_1] \quad 3.11$$

$$i(t) = \frac{dQ}{dt} = \frac{d}{dt}[\epsilon_{33}E + d_{31}T_1]wL \quad 3.12$$

The equation of current can be transformed into the complex domain using a Laplace transform, allowing for easier interpretation. The Laplace transform of a time derivative with initial conditions of zero is defined as:

$$\mathcal{L}\left[\frac{d}{dt}G(t)\right] = s\tilde{G}(s) \quad 3.13$$

Where s signifies the complex variable. The solution for current becomes:

$$\tilde{I}(s) = s\tilde{Q}(s) = s[\epsilon_{33}\tilde{E}(s) + d_{31}\tilde{T}_1(s)]wL \quad 3.14$$

Introducing the solution of the stress, equation 3.5, the current can be rewritten.

$$\tilde{I}(s) = s[(\epsilon_{33} - d_{31}^2 Y_{11})\tilde{E}(s) + d_{31} Y_{11} \tilde{S}_1(s)]wL \quad 3.15$$

Defining the electric field in terms of voltage, $E = V/h$, and dividing the equation of current by the voltage, the **admittance** of the piezoelectric actuator is determined.

$$\frac{\tilde{I}(s)}{\tilde{V}(s)} = \tilde{Y}(s) = s \left[(\epsilon_{33} - d_{31}^2 Y_{11}) \frac{wL}{h} + wL d_{31} Y_{11} \frac{\tilde{S}_1(s)}{\tilde{V}(s)} \right] \quad 3.16$$

Equation 3.16 shows that the equation of admittance is made up of two parts. The first part is a group of constants that define the electrical, or actuator, component and is defined by the material constants and the geometry of the piezoelectric actuator.

$$\text{electrical(actuator)} = (\epsilon_{33} - d_{31}^2 Y_{11}) \frac{wL}{h} \quad 3.17$$

The second part of the equation of admittance designates the electro-mechanical coupling of the actuator. The electro-mechanical coupling designates the relationship between the mechanical strain and the voltage applied to the actuator, or the sensor component of the admittance.

$$\text{electro-mechanical (sensor)} = wL d_{31} Y_{11} \frac{\tilde{S}_1(s)}{\tilde{V}(s)} \quad 3.18$$

By solving the equation of admittance for zero strain, $S_I = 0$, the effect of the actuator component on the admittance is found to act as the effective capacitance of the piezoelectric material.

$$\tilde{Y}(S_1 = 0, s) = s \left[(\epsilon_{33} - d_{31}^2 Y_{11}) \frac{wL}{h} \right] = s[\text{effective capacitance}] \quad 3.19$$

The effective capacitance will be defined as the capacitance, C , of the actuator. The effective capacitance is made up of dielectric, piezoelectric and elastic properties of the piezoelectric actuator. As a note: the capacitance quoted by most manufacturers is defined only by the dielectric properties of the piezoelectric actuator. In this paper, capacitance will refer to the effective capacitance, C , defined in equation 3.19. The equation of admittance can be rewritten as:

$$\tilde{Y}(s) = s \left[C + wLd_{31}Y_{11} \frac{\tilde{S}_1(s)}{\tilde{V}(s)} \right] \quad 3.20$$

Equation 3.20 shows the admittance is composed of the effective capacitance, designated by the constant C , and the electro-mechanical term or sensor component. The electro-mechanical term, as defined in equation 3.18, is a function of the ratio of actuator strain to applied voltage. The solution for the electro-mechanical term is determined by the boundary conditions acting on the actuator. The solution of the strain of a piezoelectric actuator bonded to a structure is now investigated.

3.2 Actuator Strain

The actuator strain is determined by the interaction of the actuator and host structure. The strain of the actuator is assumed to be the strain of the beam at the actuator bond; therefore, the strain of the actuator is determined from the equation of motion of the actuator and host structure. The equation of motion will include the dynamics of the

structure, the actuators bonded to the structure, the force input of the actuator and the external force acting on the structure. For simple beam or plate-like structures, a Rayleigh-Ritz model can be applied to determine the equation of motion of the structure with piezoelectric actuators. (23)

As the structure becomes more complex, the solution of this relationship becomes more difficult to determine. For instance, the motivation behind this research is to characterize the power requirements of the PARTI wing which consists of 72 individual actuators acting on a complex, plate-like structure (Figure 1.4). A model of the coupled motion of each individual actuator acting on the wing during active control would be necessary to solve the equation of motion. The model would include an estimate of the actuator force acting on the wing, an estimate of the external force, which is both random and non-stationary, and an estimate of the response of the wing to these forces. Also, a closed-loop control scenario must be applied to the model to simulate active vibration control. The time and energy required for this solution would be extensive and questionably accurate.

To build a better understanding of the effects of the strain to voltage response of the actuator and host structure on the admittance, a single-degree-of-freedom model is investigated. The simplified model allows for a more straightforward investigation that can later be applied to more complex structures. Thus, the beam with piezoelectric actuators is simplified as a SDOF mass, spring damper system. (Figure 3.3)

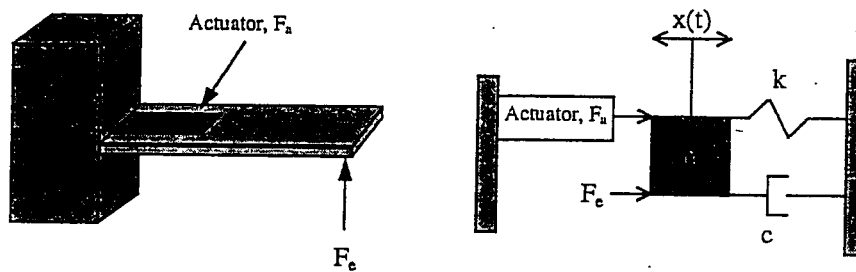


Figure 3.3: Simplification of Cantilever Beam to SDOF Structure.

First, the equation of motion of the SDOF structure in Figure 3.3 will be developed. Then the strain of the actuator will be determined from the equation of motion before investigating the specific case of active control.

3.2a Structural Equation of Motion

For a single degree of freedom system excited by an external force and a piezoelectric actuator, the equation of motion of the structure is:

$$m\ddot{x} + c\dot{x} + kx = F_a + F_e \quad 3.21$$

Where m , c , and k represent the mass, damping, and stiffness of the host structure accordingly. The actuator force is designated by F_a and the external force is designated by F_e . The mass and damping contributions of the piezoelectric actuator are assumed to be negligible. The force of the actuator is determined by the constitutive equation of stress (equation 3.5):

$$F_a = -T_1 \times Area = Y_{11}(d_{31}E - S_1)wh \quad 3.22$$

The force of the actuator acting on the structure is made up of two parts. The first is the blocking force of the actuator:

$$F_{blocking} = wd_{31}Y_{11}V \quad 3.23$$

The second part is due to the elastic stiffness of the actuator, or the Hooke's Law relationship:

$$F_{elastic} = -whY_{11}S_1 \quad 3.24$$

The next section will discuss how the blocking force and elastic force of the piezoelectric actuator couple with the host structure.

3.2b Equation of Motion and Actuator Strain

It is assumed that the bond between the actuator and structure is perfect. For this case, the strain of the actuator is assumed to be the same as the strain of the host structure where the actuator is bonded.

$$S_1 = \frac{\Delta L}{L} = \frac{x}{L} \quad 3.25$$

Equation 3.25 can then be applied to the elastic force of the actuator, the motion of the actuator in terms of the motion of the host-structure.

$$F_{elastic} = -\frac{wh}{L}Y_{11}x = -k_a x \quad 3.26$$

The constant, k_a , designates the effective stiffness the actuator contributes to the host-structure. The equation of motion of the actuator-host structure (Equation 3.21) can be rewritten:

$$m\ddot{x} + c\dot{x} + (k + k_a)x = F_{blocking} + F_e \quad 3.27$$

The normalized equation of motion is:

$$\ddot{x} + 2\xi\omega_n\dot{x} + \omega_n^2x = (F_{blocking} + F_e) / m \quad 3.28$$

The solution for the equation of motion can be determined by taking the Laplace transform of Equation 3.28:

$$\tilde{x}(s) = \frac{1}{m(s^2 + 2\xi\omega_n s + \omega_n^2)} (\tilde{F}_{blocking}(s) + \tilde{F}_e(s)) \quad 3.29$$

Using Equation 3.25 to define the strain of the actuator with the motion of the host structure, the strain of the actuator is determined.

$$\tilde{S}_1(s) = \frac{1}{mL(s^2 + 2\xi\omega_n s + \omega_n^2)} (\tilde{F}_{blocking}(s) + \tilde{F}_e(s)) \quad 3.30$$

Applying the definition of the actuator blocking force and dividing by the voltage, the ratio of strain to voltage is determined.

$$\frac{\tilde{S}_1(s)}{\tilde{V}(s)} = \frac{1}{mL(s^2 + 2\xi\omega_n s + \omega_n^2)} (wd_{31}Y_{11} + \frac{\tilde{F}_e(s)}{\tilde{V}(s)}) \quad 3.31$$

As was expected from Equation 3.31, it can be concluded that the strain to voltage ratio is a function of the motion of the actuator-host structure in response to the control force of the piezoelectric actuator and the external disturbance force.

Instead of solving for the explicit solution, two cases of structural control are investigated, perfect and imperfect control, to gain a better understanding of the electro-mechanical interaction between the actuator and the host structure.

3.3 Structural Control

The solution would traditionally be determined by solving the strain to voltage relationship developed in the previous section, Equation 3.31, which is applied to the equation of admittance, Equation 3.20. Instead, two cases of structural control are investigated, perfect control and imperfect control. "Perfect" structural control refers to the ideal case where strain throughout the structure is completely suppressed. "Imperfect" control refers to the more realistic case where strain throughout the structure is not completely suppressed. Investigation of these two cases will reveal that an upper and lower bound on the admittance can be defined. The analysis will show that the maximum power is consumed when the structure is "perfectly" controlled; and as control authority is lost, the power requirements will decrease. A minimum admittance is defined by the structural strength of the piezoelectric actuator, which corresponds to the worst case control scenario.

3.3a Perfect Control

As mentioned above, for a perfectly-controlled structure, the strain throughout the host structure is equal to zero. As indicated by Equation 3.25, the strain of the actuator will equal zero for this case. The actuator and host structure strain are equal to zero when the force generated by the piezoelectric actuator is equal and opposite to the external force as shown in Equation 3.30:

$$wd_{31}Y_{11}\tilde{V}(s) = -\tilde{F}_e(s) \quad 3.32$$

The maximum commanded force of the piezoelectric actuator is defined by the maximum blocking force:

$$\text{maximum } \tilde{F}_a(s) = wd_{31}Y_{11}\tilde{V}_{\max}(s) \quad 3.33$$

The maximum voltage, $\tilde{V}_{\max}(s)$, can be defined by two limitations, the limitation of the actuator or the limitation of the controller. The limitation of the actuator is the breakdown voltage of the piezoelectric material. The breakdown voltage is the voltage that will destroy the piezoelectric material. The maximum voltage may also be defined by the limitations of the controller, or the maximum voltage the controller can supply to the actuator.

For perfect control, the external force must be less than or equal to the maximum actuator blocking force:

$$|F_e| \leq |\max(F_u)|$$

or

3.34

$$\tilde{F}_e(s) \leq wd_{31}Y_{11}\tilde{V}_{\max}(s)$$

Substituting this relationship into Equation 3.31, the strain becomes zero. Consequently, the admittance of the piezoelectric actuator reduces to:

$$\frac{\tilde{I}(s)}{\tilde{V}(s)} = \tilde{Y}(s) = s(\epsilon_{33} - d_{31}^2Y_{11})\frac{wL}{h} = sC \quad 3.35$$

As mentioned earlier, the constant C in Equation 3.35 is the effective capacitance of a piezoelectric actuator.

3.35 Imperfect Control

If the external force exceeds the maximum blocking force, control is less than perfect. In which case, strain in the structure is greater than zero.

$$wd_{31}Y_{11}\tilde{V}_{\max}(s) < -\tilde{F}_e(s) \Rightarrow \text{strain, } S_1 > 0 \quad 3.36$$

By redefining the external force as a combination of the actuator blocking force and an additional force, f_e , as illustrated in Figure 3.4, the equation for the strain to voltage ratio can be redefined in terms of the additional force that exceeds the capacity of the piezoelectric actuators.

$$\tilde{F}_e(s) = -(wd_{31}Y_{11}\tilde{V}_{\max}(s) + \tilde{f}_e(s)) \quad 3.37$$

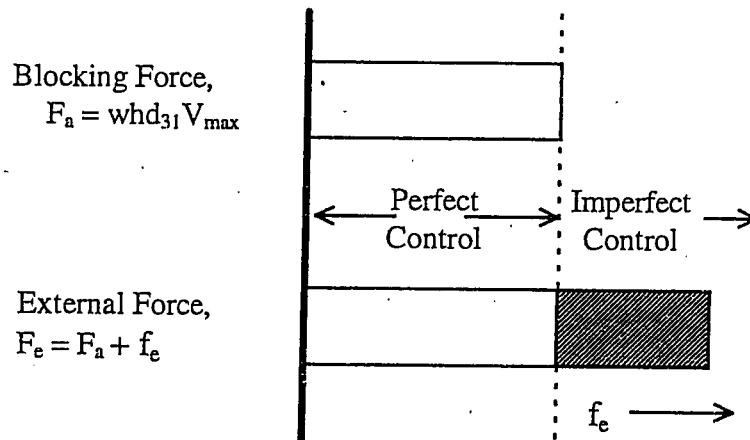


Figure 3.4: Diagram of Actuator and External Force.

The transform of the strain to voltage (Equation 3.31) can be simplified as:

$$\frac{\tilde{S}(s)}{\tilde{V}(s)} = \frac{-\tilde{f}_e(s)}{\tilde{V}_{\max}(s)} \frac{1}{mL(s^2 + 2\xi\omega_n s + \omega_n^2)} \quad 3.38$$

Applying this to the equation of admittance (Equation 3.20), the admittance for

"imperfect" control is:

$$\tilde{Y}(s) = s \left[C - \frac{\tilde{f}_e(s)}{\tilde{V}_{\max}(s)} \frac{wd_{31}Y_{11}}{m(s^2 + 2\xi\omega_n s + \omega_n^2)} \right] \quad 3.39$$

The first important detail to notice is the 180 degree phase shift between the added force, f_e , and the excitation voltage which is designated by the negative sign before the force to voltage ratio. This relationship is logical because the excitation voltage is designated to oppose the force by the control law defined in Equation 3.33. Thus, the magnitude of the

added force, f_e , actually reduces the total admittance of the actuator. Accordingly, assuming that the maximum capability of the piezoelectric actuator is used for control, as control effectiveness decreases, admittance (and thus power) decreases.

3.3c Boundaries on Admittance

From the relationship defined above, an upper and lower bound for admittance can be defined. For perfect and imperfect control, the admittance is defined as:

Perfect Control	Imperfect Control
$\tilde{Y}_{perfect}(s) = sC$	$\tilde{Y}_{imperfect}(s) = s \left[C - \frac{\tilde{f}_e(s)}{\tilde{V}_{max}(s)} \frac{wd_{31}Y_{11}}{m(s^2 + 2\xi\omega_n s + \omega_n^2)} \right]$

Thus, the maximum admittance is defined for the perfect control scenario:

$$\tilde{Y}_{max}(s) = sC \tag{3.40}$$

From the imperfect control section, the admittance will decrease as structural control is lost (or f_e increases). From Equations 3.38 and 3.39, the admittance will decrease the most at the maximum strain to voltage ratio.

$$\tilde{Y}_{min}(s) = s \left[C - wLd_{31}Y_{11} \left(\frac{\tilde{S}_1(s)}{\tilde{V}(s)} \right)_{max} \right] \tag{3.41}$$

The negative sign in Equation 3.41 corresponds with the phase shift defined in Section 3.3b.

To determine the lower bound on the admittance, the maximum strain to voltage ratio must be determined. The maximum strain is determined by the ultimate strength of the piezoelectric material. If the strain in the piezoelectric actuator exceeds the ultimate strength of the material, the actuator will fail and power will no longer flow through the actuator. The voltage is determined by the control law. However, assuming the capacity of the piezoelectric actuators is exhausted and V_{max} is used, then the maximum strain to voltage ratio is defined by:

$$\left(\frac{\tilde{S}(s)}{\tilde{V}(s)} \right)_{MAX} = \frac{-\tilde{S}_{failure}(s)}{\tilde{V}_{max}(s)} \quad 3.42$$

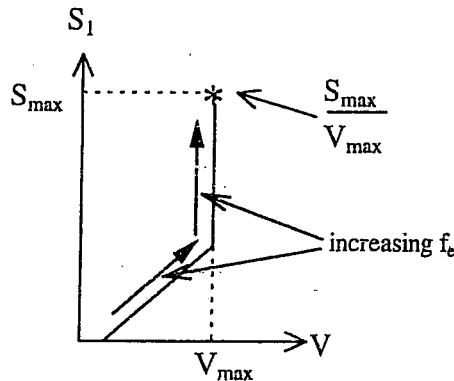


Figure 3.5: Strain and Voltage Relationship for Active Control

Applying this relationship back into the equation of admittance for imperfect control (Equation 3.39):

$$\tilde{Y}_{min}(s) = s \left[C - wLd_{31}Y_{11} \frac{\tilde{S}_{failure}(s)}{\tilde{V}_{max}(s)} \right] \quad 3.43$$

The lower boundary of the admittance is now defined. The most important detail to notice is that both the upper bound and the lower bound of the admittance are defined

independent of the dynamics of the host structure. Thus, the admittance of a piezoelectric actuator can be estimated within a region for active vibration control. For example, using an ACX QP40W PZT actuator (Appendix 3), the percent difference between the best and worst case for the admittance is determined.

$$\text{percent difference} = \frac{wLd_{31}Y_{11} \frac{\tilde{S}_{failure}(s)}{\tilde{V}_{max}(s)}}{C} \times 100\% \cong 10\% \quad 3.44$$

Even at the worst case scenario for vibration control, there is only a 10% reduction in admittance. Thus, the boundaries for the admittance are defined between the equation for perfect control, Equation 3.35, and the minimum admittance, Equation 3.43. Thus, for most control situations, a conservative estimate of the admittance can be made by neglecting the influence of the additional external force, f_e . Note, the above estimate of admittance assumes two things; the actuator is excited at the maximum voltage and that the actuators is used for vibration control. This estimate of error is not valid unless these conditions are met. The estimate of admittance is now defined and can be applied to the equation of power mentioned earlier.

$$\tilde{Y}_{estimate}(s) \cong sC \quad 3.45$$

Where this estimate is always greater than the actual admittance with greater than 90% accuracy for active vibration control.

3.4 Piezoelectric Power Required for Active Control

This section will present the equations for predicting the power required of piezoelectric actuators during active vibration control. Additional considerations associated with piezoelectric power are also discussed. Conservative calculations of the power consumption of piezoelectric actuators can be determined without direct consideration of the dynamics of the actuator and host structure. The results of Section 3.3 indicate that the admittance can be determined with greater than 90% accuracy by neglecting these dynamics. Transforming Equation 3.45 from the complex domain to the frequency domain, the admittance becomes:

$$Y(\omega) = j\omega(\epsilon_{33} - d_{31}^2 Y_{11}) \frac{wL}{h} = j\omega C \quad 3.46$$

$$\text{phase angle, } \varphi = \tan^{-1} \left[\frac{\text{Im}[Y(\omega)]}{\text{Re}[Y(\omega)]} \right] = \frac{\pi}{2}$$

Transforming the admittance back to the time domain and solving for the current:

$$I(t) = C \frac{\partial V}{\partial t} \quad 3.47$$

For a voltage signal with sinusoidal motion, $V(t) = V \sin(\omega t)$, the power becomes:

$$P(t) = \frac{1}{2} \omega C V \sin(2\omega t) \quad 3.48$$

Equation 3.48 is a conservative estimate of the piezoelectric power consumption for active control given the capacitance of the actuator and the voltage and frequency of the

control law output signal. The capacitance of the actuator is determined from Equation 3.19. For multiple piezoelectric actuators connected in parallel, the total capacitance is the sum of the capacitance of each piezoelectric actuator:

$$C_{total} = \sum_{i=1}^n C_i \quad 3.49$$

C_i = Effective Capacitance of Actuator i

n = Number of Actuators Being Used

The ability to predict the maximum power consumption of piezoelectric actuators can be extremely useful in the design of structures that will use piezoelectric actuators for active control. For example: once an estimate of the number and type of piezoelectric actuators are established; the magnitude of the maximum power required to control vibration on a large airplane wing can be calculated as follows:

$$P_{max}(\omega) = \frac{1}{2} \omega_{max} V_{max}^2 \sum_{i=1}^n C_i \quad 3.50$$

Where ω_{max} is the maximum frequency of the control law output signal. Generally, this frequency is defined by the frequency of the highest mode of interest for control purposes.

V_{max} is the maximum voltage that can be applied to the actuators. This is determined by either the maximum voltage the piezoelectric actuators can withstand, or the maximum voltage the controller can generate.

The benefits of this analysis can be seen in Equation 3.48 and 3.50 where there is no dependency on the structural dynamics between the actuator and host structure. The computational effort in characterizing the power requirements of a piezoelectric actuator during active control are drastically reduced from previous models of piezoelectric power. Making the application and development of piezoelectric technology more accessible.

An additional consideration in calculating power is that traditional power amplifiers are not designed for a capacitance load like that of piezoelectric actuators. For this reason, the total power consumption is based on the combined magnitude of the imaginary power and real power, or the apparent power. A detailed description of imaginary and real power is given in Appendix 1. As noted in the introduction, a new generation of power amplifiers are being developed that are capable of storing the imaginary power, or the power load of a piezoelectric actuator. The only power loss would be due to losses within the amplifier, actuator and circuitry. Thus, application of the new generation of power amplifiers may prove to be a drastic reduction in piezoelectric power consumption. Linear amplifiers are the most dependable and widely used amplifier at this time.

Note: the above developments assume the capacitance of piezoelectric actuators is constant with respect to voltage. Although this assumption is commonly made, the experimental tests conducted as a part of the current research show that capacitance actually increases with voltage. Thus, to accurately predict the power consumption using Equation 3.48 or 3.50, the measured capacitance of the piezoelectric actuators must be used. Further description of this phenomena is discussed in the Experimental Verification chapter that follows.

CHAPTER 4: EXPERIMENTAL VERIFICATION

4.0 Introduction to Experimental Verification

This chapter focuses on the experimental verification of the previous analytical development. The conclusion of the analysis is that for active vibration control piezoelectric admittance can be determined without modeling the actuator and host structure's dynamics. The admittance can then be applied to the equation of power to determine the power characteristics of the piezoelectric actuators utilized for active vibration control.

During the experimental verification of the analysis, a non-linearity in the material properties of the piezoelectric actuator was discovered. The non-linearity will be discussed before the results of the experimental verification are presented because an understanding of the non-linearity is vital to interpreting the experimental results.

The verification of the analytical results will be presented for three cases: open-loop excitation, feed-forward control and closed-loop control cases. During open-loop excitation, the piezoelectric actuators are being used to excite motion in the structure without feedback. During feed-forward and closed-loop control, an external disturbance is applied by a force shaker and the piezoelectric actuators actively inhibit the motion in the structure using feed-forward or feedback control laws.

4.1 Single-Degree-Of-Freedom Test Structure

For the experimental tests, a single-degree-of-freedom model was used (Figure 4.1). The model is a 12 inch long cantilevered beam made of an aluminum honeycomb core sandwiched between graphite-epoxy face sheets. An aluminum mass was fixed to the tip of the beam to isolate the first bending mode, simulating a single-degree-of-freedom (SDOF) system. The aluminum mass reduced the natural frequency of the first bending mode of the beam to a frequency that made data acquisition and analysis of the data more convenient. The piezoelectric actuators were adhered at the root of the beam because the root of the beam is the region of highest curvature in the first bending mode.

Piezoelectric actuators are essentially strain actuators and have been shown to have the most control effectiveness in the region of highest curvature. Two ACX type QP-40W PZT actuators (Appendix 3) were used. The actuators were adhered to the beam in the same orientation as illustrated in the introductory section in Figure 1.3.

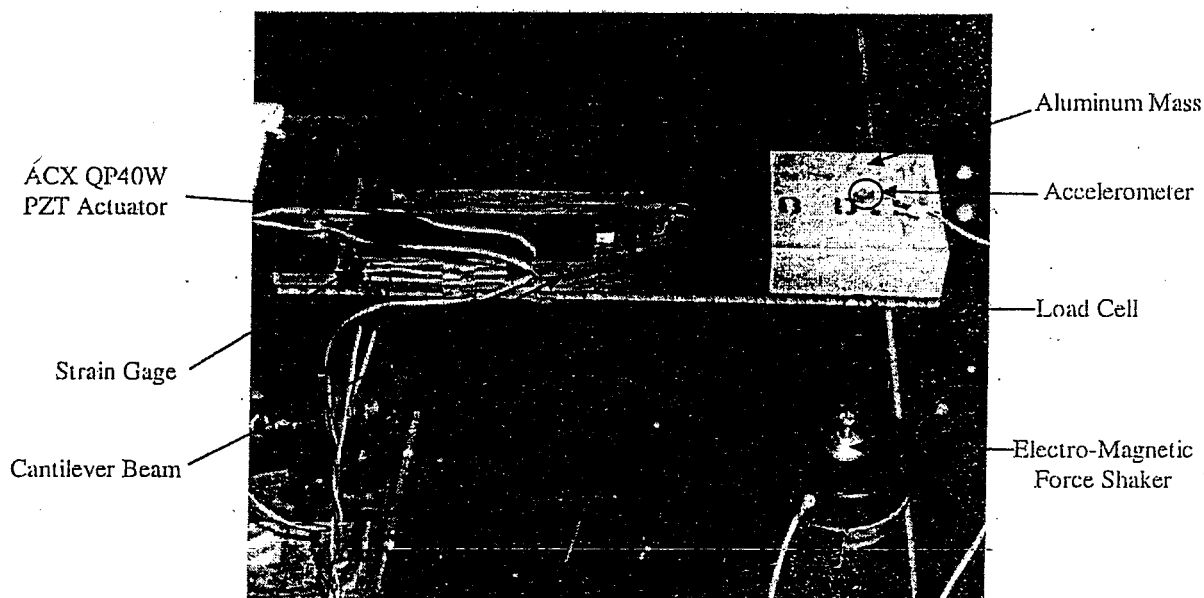


Figure 4.1: Picture Of Single-Degree-of-Freedom Test Structure

During closed-loop testing, the external force was introduced by applying an electro-magnetic force shaker that was orientated to supply a force at the center of gravity of the aluminum mass. Force output of the shaker was measured through a load cell at the tip of the stinger connecting the shaker to the structure. A strain gage was adhered adjacent to the piezoelectric actuators at the root of the beam to measure strain in the beam. An accelerometer was positioned at the center of gravity of the aluminum mass to measure tip acceleration. An ammeter was used to measure the current in the piezoelectric actuator circuit. (Figure 4.2)

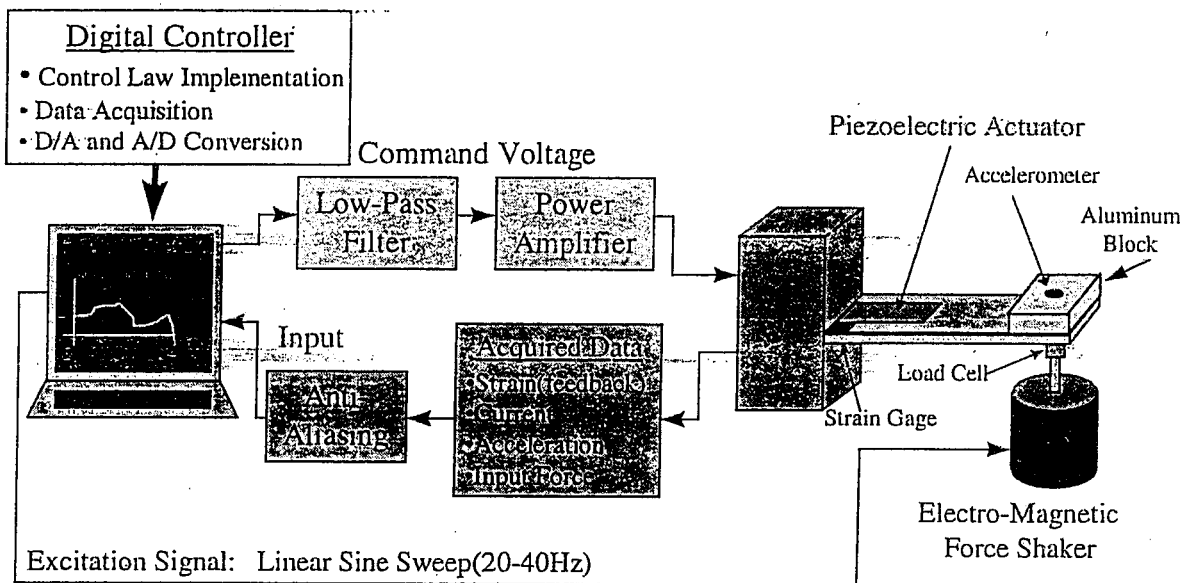


Figure 4.2: Illustration Of Test Setup

Data acquisition and control was performed using an SGI workstation. The signal used to command the piezoelectric actuator was generated at 2 kHz and then passed through a low-pass filter with a cut-off frequency of 1000 Hz. Filtering the excitation signal was necessary due to the response of the piezoelectric actuator to a digitally generated

excitation signal with a sampling rate below the bandwidth of the piezoelectric actuator. Digitally generated signals resemble a staircase in structure, or a step input at each time step. Although, this does not typically influence the control effectiveness of the actuator, the current signal becomes extremely noisy and difficult to measure if the excitation signal is not filtered. The response of the actuator to the step input of the excitation signal is a spike in the current that gives the current a "sawtooth" appearance. Current is one of the essential quantities that defines admittance; therefore, an accurate measure of the current was important in these experiments. This problem was solved by conditioning the digital signal with a low-pass filter. The result was a "smooth" excitation signal that more closely resembles an analog signal. Using a linear power amplifier, the filtered signal was amplified with a gain of 17. Further discussion of the amplifier types and characteristics will be introduced in Section 4.6. Data acquisition is performed at a sampling rate of 250 Hz yielding a Nyquist frequency of 125 Hz. An anti-aliasing filter was implemented with a cut-off frequency of 100 Hz.

4.2 Non-Linear Capacitance

As noted previously, experimental tests revealed a non-linear characteristic in the capacitance of the piezoelectric actuator. Brief mention of this phenomenon was made by Warkentin (24) and a more detailed investigation was recently presented by Sherrit (25).

Experimental tests revealed that the capacitance of the piezoelectric actuators increases with voltage as indicated from Figure 4.3. Capacitance was measured by clamping the host structure to inhibit all motion. Recalling from the equation of admittance, when the strain is zero, the admittance is a function of frequency and capacitance alone. The

capacitance of the piezoelectric actuator is measured from the slope of the admittance versus frequency plot.

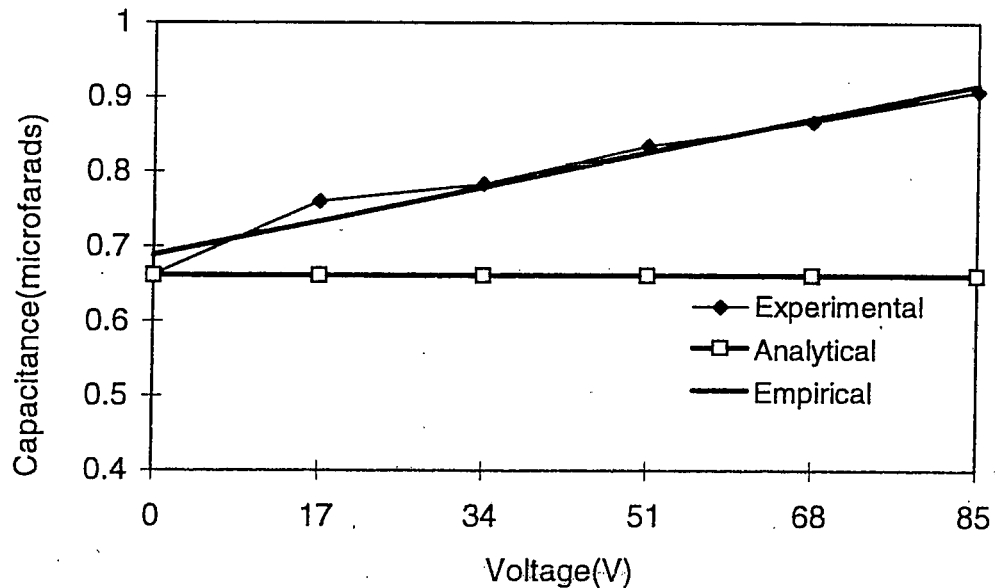


Figure 4.3: Capacitance vs. Excitation Voltage for The Actual, Analytical and the Empirical Model of Capacitance.

An empirical model of capacitance as a function of voltage was developed to model the varying capacitance behavior. This was done by performing a first order least squares approximation on the experimentally determined values of capacitance. The results found a 0.44% increase in capacitance per volt. Resulting in an empirical model of capacitance:

$$C_{empirical} = C_0 + \frac{\partial C}{\partial V} V(\omega) \quad 4.1$$

$$C_0 = 0.661 \mu\text{Farads}$$

$$\frac{\partial C}{\partial V} = (0.0044)C_0$$

Piezoelectric actuators are commonly operated in the 100 to 200 volt range. In this volt range, approximately a 40-90% increase in capacitance can be expected over the manufacturer's quoted value. The manufacturer's quoted value of capacitance is shown in Figure 4.3 as the analytical value, 0.661 μ Farads.

The empirical solution above is a linear relationship (Equation 4.1), but the effect of the non-constant capacitance makes the admittance nonlinear because the admittance is now a function of voltage as well:

$$Y(\omega) = j\omega \left[\left\{ C_0 + \frac{\partial C}{\partial V} V(\omega) \right\} - \omega L d_{31} Y_{11} \frac{\tilde{S}_1(\omega)}{\tilde{V}(\omega)} \right]$$

It is common for electrical engineers to refer to non-constant capacitance as non-linear. Not because of the relationship between capacitance and voltage, but for the non-linearity introduced in the admittance as shown above. Because the non-linearity was introduced and accounted for in the frequency domain, the analytical solution of admittance can not be transformed into the time domain. Thus, the analytical equations of power can not be determined in the time domain. This does not pose a problem in the characterization of admittance or power. There is no evidence that suggest that admittance may change with time; therefore, a sufficiently accurate model of admittance and power can be characterized in the frequency domain. However, quantifying the energy consumption of a piezoelectric actuator requires the power as a function of time. Thus, the only way to

determine energy consumption for a test is to experimentally measure the voltage and current and determine the power as a function of time directly.

The admittance is now a function of the voltage or control signal that is applied to the piezoelectric actuator, the frequency of the control law signal as well as the material properties of the piezoelectric material. It is important to realize that the admittance must be determined for individual control signals as the control signals may change between tests, control laws or boundary conditions.

During this research, efforts were made to investigate the origin of the non-linear behavior of the capacitance. Measurement techniques and meter calibration were checked and verified to be accurate. Investigations were made exploring thermal effects. The high voltages exposed to piezoelectric actuators were thought to increase the temperature within the material which may result in the change in capacitance.

Experimental test measured a change in temperature of one degree Celsius between 17 and 85 volts. Thus, thermal effects were considered negligible.

Sherrit's (25) presentation identified that the dielectric, piezoelectric and elastic constants are influenced by the voltage applied to the material and the stress acting on the material. The consequence is that the material constants will change under different boundary conditions and under different excitation signals. Some plots that illustrate the change in capacitance under different boundary conditions are found in Appendix 2. The results verify that the capacitance will change with both the boundary conditions and voltage. At this point, too many unknowns still exist to completely characterize how the material

properties of piezoelectric actuators are affected by the applied voltage or the stress acting on the actuator.

The author believes that due to the inherent nature of piezoelectric materials, changes in material properties should be expected with changes in excitation. As the material changes dimension with excitation, the molecular or ionic structure of the dipoles within the material also shift, rotate or change shape. The change in position or shape of the dipoles may change the material properties of the piezoelectric material. This is only a hypothesis with the conclusion that more research needs to be conducted to truly understand the material properties of piezoelectric materials.

4.3 Open-Loop Excitation

This section investigates the admittance during open-loop excitation. During open-loop excitation, the piezoelectric actuators are utilized to excite motion in the structure without feedback. The purpose of investigating open-loop excitation is to illustrate the effects of the phase angle between strain and voltage.

The strain response due to voltage input transfer function for a laminar piezoelectric actuator fixed to a single-degree-of-freedom structure resembles an ideal second order system. Below the natural frequency, the phase is zero degrees. Above the natural frequency, the phase is 180 degrees. This means that the ratio of strain to voltage is positive below the natural frequency and negative above the natural frequency. Inserting this strain to voltage relationship for open-loop excitation into the equation of admittance:

$$|\tilde{Y}(\omega)| = \omega \left[C + \omega L d_{31} Y_{11} \left| \frac{\tilde{S}_1(\omega)}{\tilde{V}(\omega)} \right| \right] \quad \omega < \omega_n \quad 4.2a$$

$$|Y(\omega)| = \omega \left[C - \omega L d_{31} Y_{11} \left| \frac{\tilde{S}_1(\omega)}{\tilde{V}(\omega)} \right| \right] \quad \omega > \omega_n \quad 4.2b$$

The admittance is found to increase due to the strain to voltage response for frequencies below the natural frequency and decrease for frequencies greater than the natural frequency. However, the increase and decrease in admittance will only cause minor fluctuations about the mean admittance generated by the effective capacitance, C.

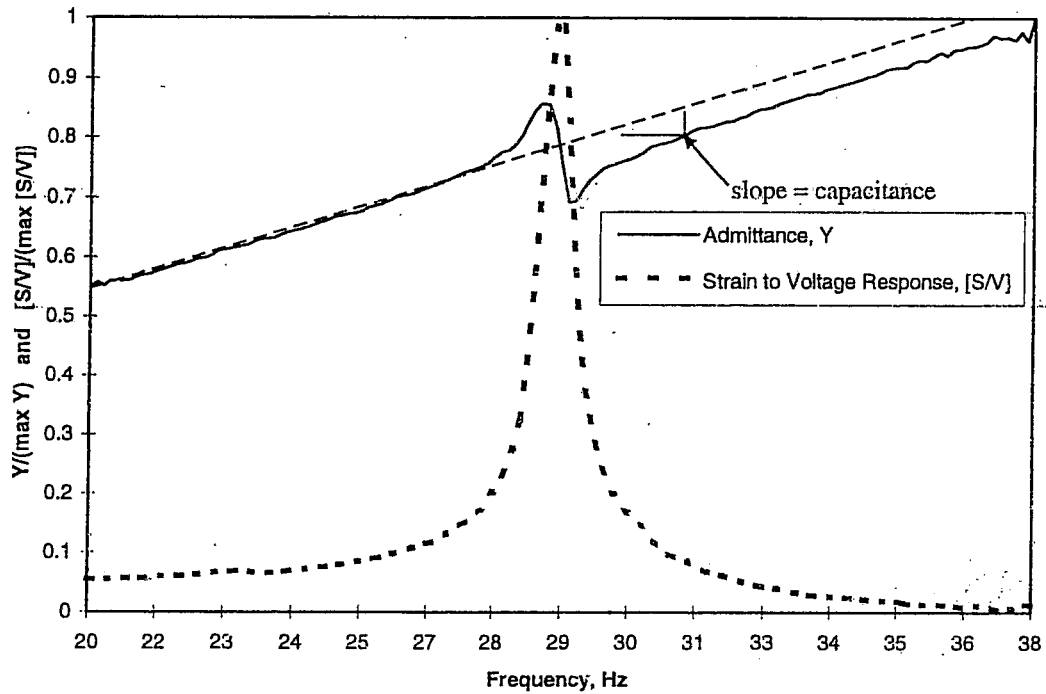


Figure 4.4: Open-Loop Excitation Response of Admittance and Strain to Voltage Response

Figure 4.4 is a comparison of the frequency response curve of strain to voltage and the admittance of the piezoelectric actuator during open-loop excitation. As predicted by

Equations 4.2a and 4.2b, the admittance is found to increase in the modal region above the mean for frequencies less than the natural frequency (29 Hz) and decrease below the mean for frequencies greater than the natural frequency. The phase relationship between the strain and excitation directly correspond to how the mechanical dynamics, $\frac{S_1}{V}$, affect the electrical admittance.

With this in mind, the control scenario should yield predictable results. The control law is designed to oppose the motion in the structure. As developed in the analysis section, the strain to voltage relationship should always be 180 degrees out of phase. Thus, the mechanical dynamics will always reduce the magnitude of the admittance.

4.4 Feed-Forward Control (constant amplitude excitation)

During feed-forward control, the piezoelectric actuator is used to inhibit motion within the structure. A diagram of feed-forward vibration control is shown in Figure 4.5. The objective of this experiment was to investigate the effects of strain on the admittance during active vibration control. Because of the non-linearity in the capacitance discussed in Section 4.2, the equation of admittance now changes.

$$|Y(\omega)| = \omega \left[\left\{ C_0 + \frac{\partial C}{\partial V} V(\omega) \right\} - \omega L d_{31} Y_{11} \left| \frac{\tilde{S}_1(\omega)}{\tilde{V}(\omega)} \right| \right]$$

Where the capacitance is replaced by Equation 4.1, and the phase relationship between the strain to voltage ratio was assumed to be 180 degrees during vibration control.

Examination of the above equation shows that a variation in the voltage will introduce a

variation in the admittance due to the non-linear capacitance. Unless the voltage, $V(\omega)$, is identical for both tests, comparing the effects of strain on the admittance from one test to the next becomes difficult. For this reason, the control law was designated to excite the piezoelectric actuators with a constant amplitude signal that is 180 degrees out of phase with the signal going to the external force shaker. This ensures that the forces of the actuators are always opposing the external force. With a constant amplitude excitation signal, the only variable in the equation of admittance was the strain, allowing for a more accurate investigation of how strain affects the admittance.

The feed-forward control was designated by breaking the excitation signal in two signals before exciting the structure. One signal is sent to the piezoelectric actuator with a constant amplitude. The poles on the second signal are switched (designating a 180 degree phase shift) and the signal is sent to the electro-magnetic force shaker. A post-gain amplifier is used to control the amplitude of the external force.

Two tests were compared, Test A and Test B. The amplitude of the excitation signal was identical for both tests so the admittance may be compared between tests. The magnitude of the external force in Test B was greater than the magnitude in Test A. The greater external force resulted in greater structural strain. With identical excitation signals to the actuator, the only change in the admittance was caused by the greater strain in Test B.

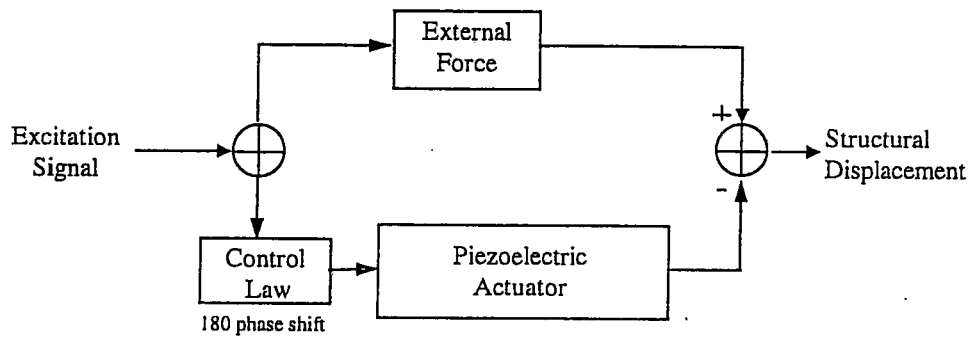


Figure 4.5: Diagram of Feed-Forward Control Law.

The excitation signal was a sine sweep between 20 and 40 Hz to ensure the first mode of the structure is excited (32 Hz). The increase in natural frequency between the open-loop excitation test (29 Hz) and the closed-loop control test (32 Hz) was due to the presence of the electro-magnetic force shaker which adds stiffness and damping to the host structure.

Open-loop excitation will refer to the case where the external force shaker is exciting motion in the structure, feed-forward control will refer to the case the piezoelectric actuators are used to inhibit the motion generated by the external force. In Test A, feed-forward control demonstrated a 53.5 % attenuation in strain from the open-loop excitation case (Figure 4.6A). Feed-forward control in Test B demonstrated a 41.5% attenuation in strain from open-loop excitation (Figure 4.6B).

Both test successfully demonstrated vibration control. The admittance between Test A and Test B can now be examined. During feed-forward control, the strain of the structure in Test B was 600% greater than the strain in Test A. The analysis predicted that an increase in strain will cause a decrease in admittance. Thus, the admittance in Test B is expected to be less than the admittance in Test A. The admittance of the piezoelectric

actuators during feed-forward control for Tests A and B are compared with the empirical model of admittance in Figure 4.7. As expected, the admittance for both tests are less than the empirical model. As expected by the analysis, the greater structural strain in Test B resulted in a greater reduction in admittance as compared to Test A.

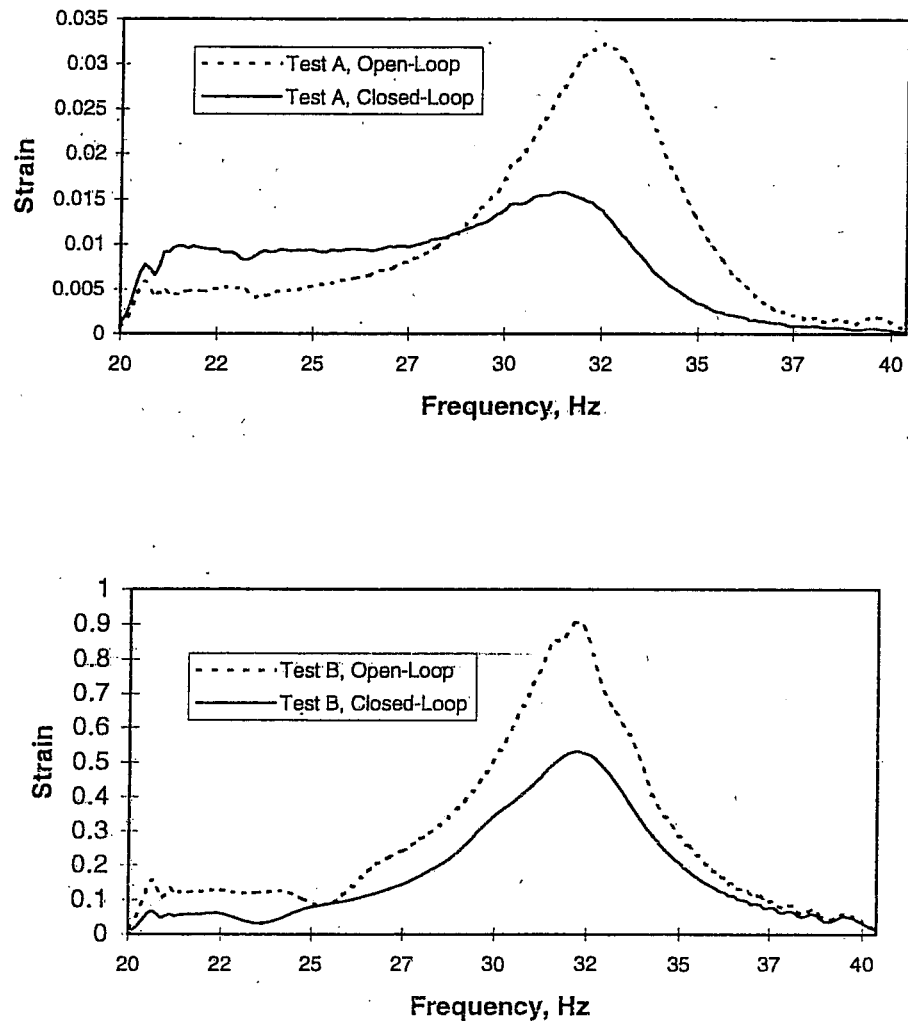


Figure 4.6 A (top) and B (bottom): The PSD of Strain for Test A and Test B With Piezoelectric Actuator On and Off.

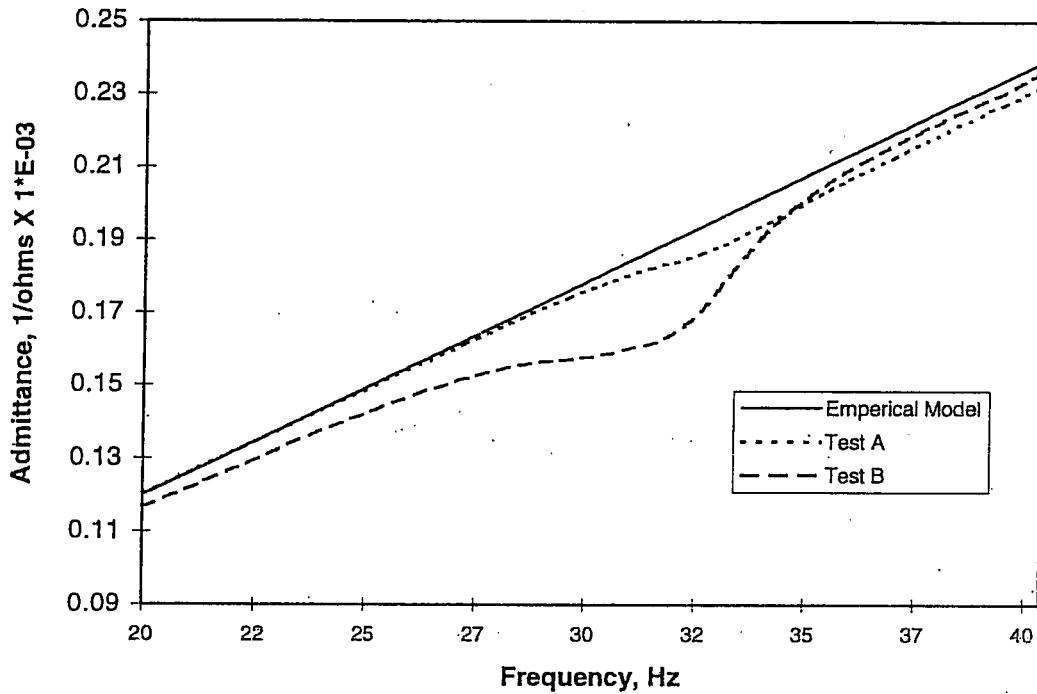


Figure 4.7: Relative Admittance Between Empirical model, Test A and Test B.

The analysis also predicted that the increase in strain would be insignificant to the overall admittance. Figure 4.8 compares the percent error between the empirical model of admittance and the experimental admittance. Again, the error in Test B is greater because of the higher strain energy in the structure. Although, the error is significantly greater in Test B (14%) than Test A (4%), it should be noted that the strain in the structure is 600% greater in Test B. Thus, a 600% increase in structural motion only increased the error in the admittance by 10%, which verifies that the mechanical dynamics, or strain, has a relatively insignificant influence on the admittance during vibration control.

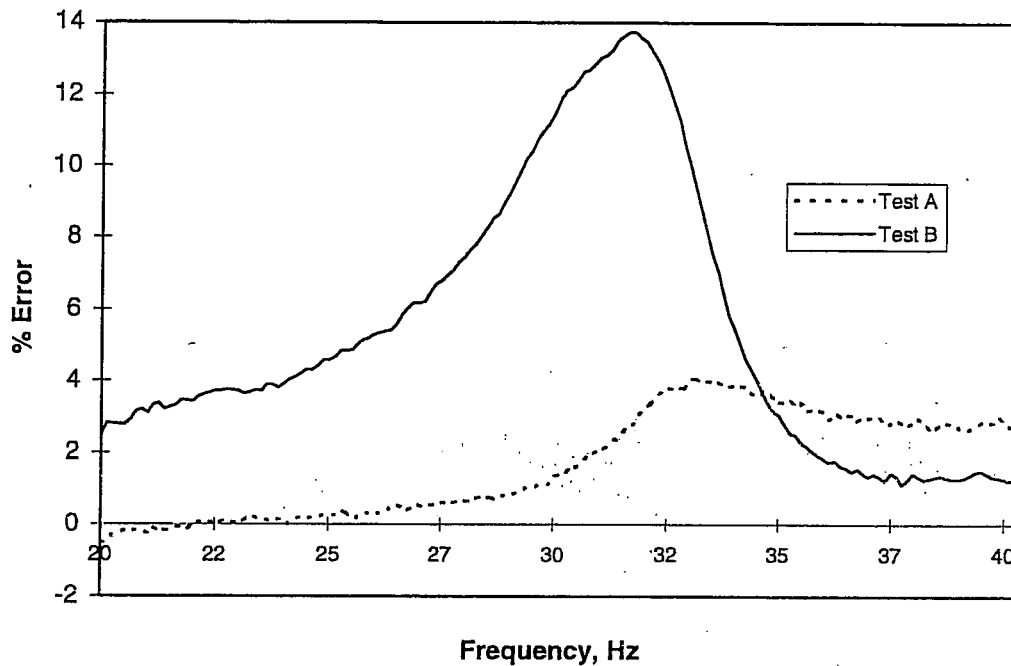


Figure 4.8: Percent Error Between the Empirical Model And Tests A and B.

Furthermore, the excitation signal utilized during both tests was only 37% of the piezoelectric actuator's maximum allowable voltage. Recalling from Equation 3.48 if the maximum voltage was supplied to the actuator, the error in the admittance could have been reduced by a factor of 3.

The important details highlighted by these tests are 1) the actual admittance of the piezoelectric actuators never exceed the empirical model of admittance that ignores the mechanical motion of the actuator and host structure and 2) a significant quantity of strain induces a small decrease in the admittance of the piezoelectric actuator. Thus, this test supports the theory developed in the analytical section that a conservative model of admittance can be determined without modeling the mechanical dynamics of the actuator

and host structure. The next experiment verifies this theory for the case of closed-loop control or active vibration control using a more realistic strain-feedback control law.

4.5 Closed-Loop Control (strain-feedback)

During closed loop-control, the piezoelectric actuators are used to inhibit motion in the structure using a feedback control law as illustrated in Figure 4.9. The addition of the control law introduces an active vibration control scheme where the control law reacts to the structural displacement, attempting to actively minimize structural displacement.

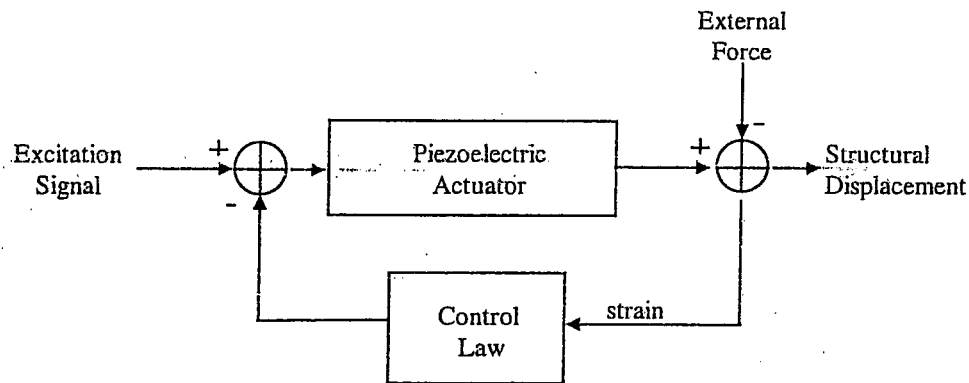


Figure 4.9: Diagram of closed-loop control law.

The digital controller is used to measure the strain in the structure at the root of the beam directly adjacent to the piezoelectric actuator. The strain is fed to the control law which generates a signal 180 degrees out of phase with the strain at an amplitude assigned by the user.

Since experimental tests showed that capacitance increases with voltage, all values for capacitance were calculated using the empirical model of capacitance, Equation 4.1. As mentioned in the previous section, the strain in the structure will reduce the admittance of

the actuator. Thus, the empirical model of admittance should always be greater than or equal to the experimental admittance measured during the test.

Two estimates of piezoelectric admittance during active vibration control are presented using Equation 4.1. Both estimates of admittance are plotted against the experimental admittance. The first estimate of admittance, as seen in Figure 4.10, assumes the control law output voltage is unknown; therefore, the maximum voltage of the actuator is used to determine the capacitance. From Figure 4.10, the maximum admittance is clearly greater than the experimental admittance. The second estimate of admittance, as seen in figure 4.11, uses the power spectral density of the control law output voltage to calculate the capacitance. This yields an estimate of the admittance for this specific control output voltage. From Figure 4.11, the estimated admittance is greater than or equal to the experimental admittance.

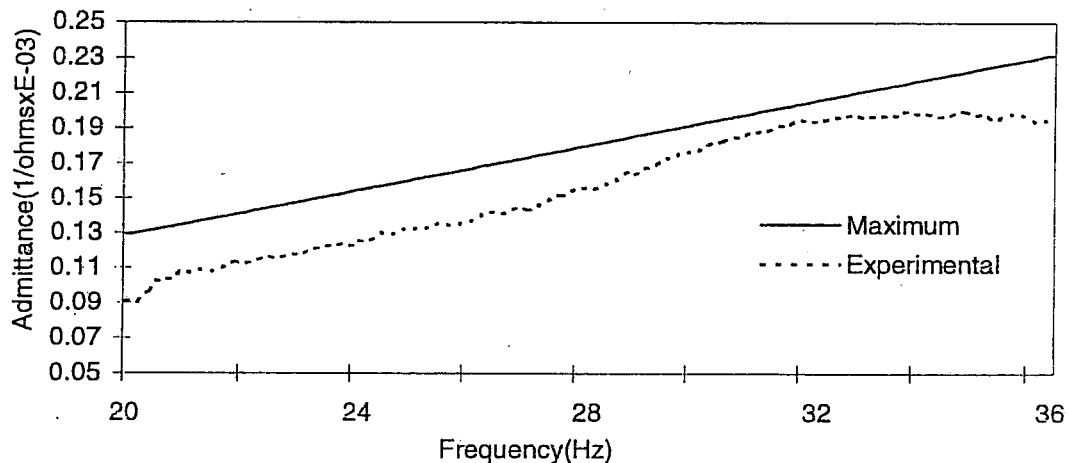


Figure 4.10: Frequency Response of Calculated Maximum Admittance and Experimental Admittance.

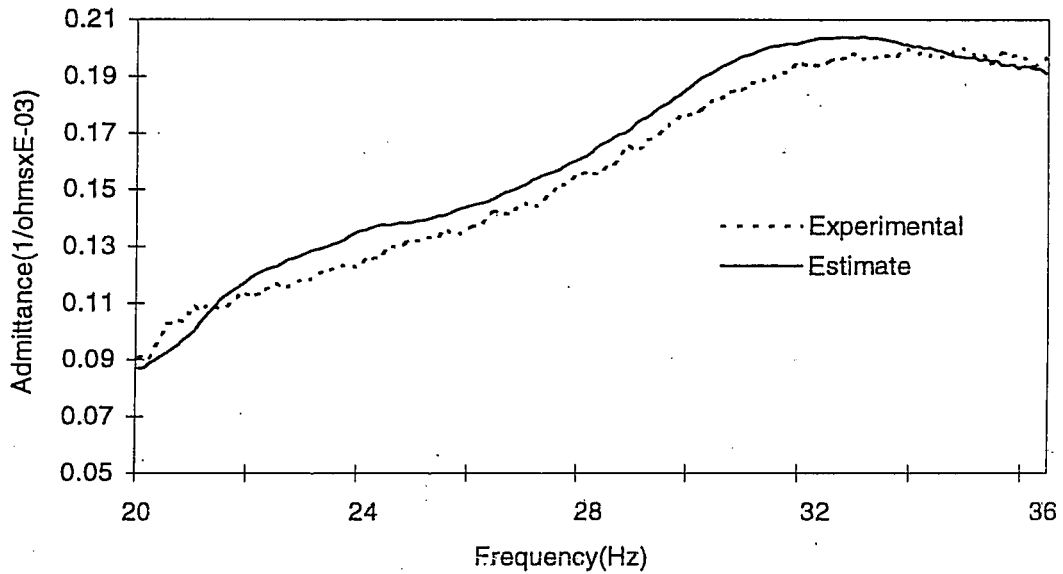


Figure 4.11: Frequency Response of Estimated Admittance and Experimental Admittance.

This is consistent with what was stated in Section 3.4. The control law used for this example displayed a 20% reduction in structural vibration, or 80% of the strain energy still exists. For this control law, the difference between the experimental and the estimated admittance was never greater than 3%. Thus, the structural motion has a negligible effect on the total admittance of the piezoelectric actuator for active vibration control. The admittance is greater than the estimate at the ends of the frequency range due to an abrupt loss of frequency content, or a problem referred to as Gibb's phenomenon.

With an estimate of admittance, the power required by the piezoelectric actuator for active vibration control can easily be calculated. Using Equation 3.2, the power is determined in the frequency domain (Figure 4.12)

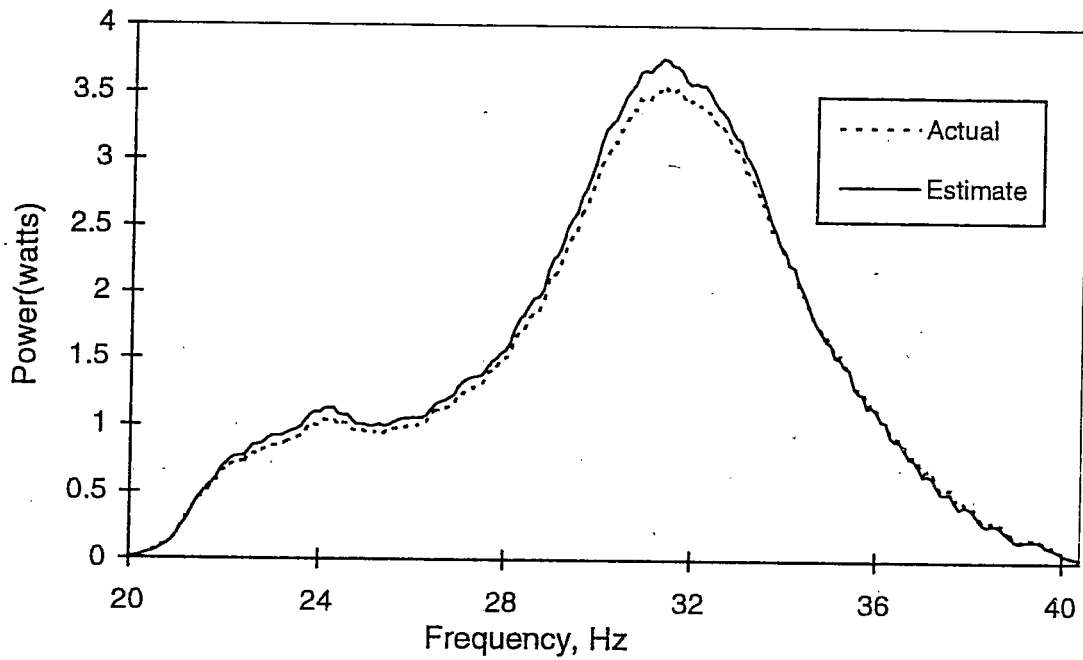


Figure 4.12: Plots of Actual Power and Estimated Power vs. Frequency.

As expected; the estimate of power is greater than or equal to the actual power across the entire bandwidth. Also, the error is insignificant (less than 3%) across the bandwidth.

CHAPTER 5: CONCLUSION

Analytical models of piezoelectric power consumption during active vibration control were developed. These developments showed that piezoelectric power consumption is essentially a function of the material and geometric properties of the piezoelectric actuators. The structural dynamics of the host structure and actuator have a minimal effect on the power consumed by the actuators and in fact, will reduce the power consumed by piezoelectric actuators. Thus, maximum power is consumed when the vibration of the host structure is completely controlled.

A single-degree-of-freedom experimental model was used to verify that a conservative estimate of power consumption can be made by ignoring structural dynamic effects. Verification of the analysis was performed using two cases of closed-loop vibration control. Both test cases verified the results. Also, it was verified that the effect of increased strain reduces admittance. The experimental results showed that even with large quantities of strain in the structure and the actuator, the admittance was reduced an insignificant amount and the analytical model of admittance was always greater than the admittance measured during the experiment. The experimental verification also revealed a non-linearity in the capacitance of the piezoelectric material. The non-linearity was accounted for with an empirical model. Without the empirical model, the error in the estimate of admittance and power could be 40% to 90% within the actuator operating range. Note, these conclusions are only valid for vibration control using piezoelectric actuators and do not apply to open-loop excitation.

The analysis also showed that the electrical load of the piezoelectric actuator is predominantly a capacitor. Because capacitors create a reactive electrical load, the type of power amplifier used will greatly influence the total power consumption of the piezoelectric actuator. In addition to examining piezoelectric power consumption, this research revealed a non-linear behavior in the material properties of piezoelectric materials. Future work includes a characterization of piezoelectric material properties with a concentration on defining the material non-linearity, validating the power consumption results using multiple-degree-of-freedom experimental models, and an investigation of piezoelectric actuator self-sensing capabilities for feedback control laws.

APPENDIX-1: Electrical Analysis:

A short introduction to the tools required for electrical analysis will be presented. An understanding of the fundamentals behind electrical engineering is required to understand the characterization of electrical power consumption.

A-1.1a Definitions (Reference 27)

Table A-1.1 Important Electrical Quantities

Quantity	Symbol	Definition	Unit	Abbreviation	(alternate)
Energy	w	ability to do work	joule	J	(N*m)
Power	p	energy/unit time	watt	W	(J/s)
Charge	q	quantity of electricity	coulomb	C	(A*s)
Current	i	rate of flow of charge	ampere	A	(C/s)
Voltage	v	energy/unit charge	volt	V	(W/A)
Electric Field	E	force/unit charge	volt/meter	V/m	(N/C)
Resistance	R	voltage/unit of current	ohms	Ω	1/siemens
Capacitance	C	current/time rate of change of voltage	farads	F	

Power measures the rate at which energy is transferred. Power is defined by the time rate of change of energy and is measured in units of watts.

$$p = \frac{dw}{dt}$$

A-1.1

Charge is the quantity of electricity. Charge is defined as conservative because it can neither be created or destroyed and is measured in units of coulombs.

The **current** through an area is defined by the electric charge passing through the area per unit time and is measured in units of amperes.

$$i = \frac{dq}{dt} \quad \text{A-1.2}$$

Voltage is a measure of electrical potential difference. The energy-transfer capability of a flow of electric charge is determined by the voltage. Voltage is defined by the quantity of energy per unit charge and is measured in volts.

$$v = \frac{dw}{dq} \quad \text{A-1.3}$$

Resistance is a measure of the conductance of a material. It is defined by the ratio of voltage to current and is measured in units of ohms.

$$R = \frac{v}{i} \quad \text{A-1.4}$$

Conductivity is the inverse of resistance.

Capacitance defines the ability of a material to store a charge. The current in a capacitor is found to be proportional to the time rate of change of the applied voltage.

$$i = C \frac{dv}{dt} \quad \text{A-1.5}$$

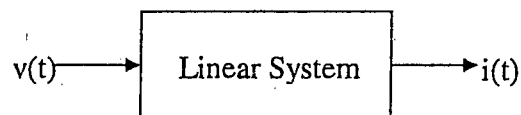
Material capacitance is defined by the permittivity, ϵ , of the material and its geometry.

$$C = \epsilon \frac{\text{area}}{\text{thickness}} \quad \text{A-1.6}$$

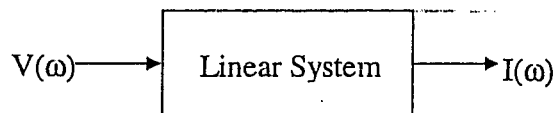
These definitions make up a small part of electrical engineering but will be sufficient in the analysis of the power requirements of piezoelectric actuators. A brief introduction to electrical analysis is introduced and will then be applied to piezoelectric actuators.

A-1.1b Electrical Analysis (Reference 27)

Consider the linear system:



Where the voltage and current are related through the convolution integral. This system can be transferred into the frequency domain.



Where the relationship can be expressed linearly using the frequency response function, $Y(\omega)$.

$$I(\omega) = Y(\omega)V(\omega) \quad \text{A-1.7}$$

In this case, the frequency response function, $Y(\omega)$, is defined as the **admittance** of the circuit. Because of the relative ease of applying a linear system in the frequency domain, admittance is commonly used in defining the characteristics of electrical circuits. The

units of admittance are 1/ohms or siemens. Admittance generally defines the conductance of a circuit with frequency content.

Impedance is also commonly used to define the linear relationship between current and voltage.

$$V(\omega) = Z(\omega)I(\omega) \quad \text{A-1.8}$$

The impedance, $Z(\omega)$, of a circuit is the inverse of the admittance with units of ohms.

Impedance defines the resistance of a circuit with frequency content. Both admittance and impedance are often complex functions, for this reason, admittance and impedance are defined in terms of magnitude and phase.

$$\text{magnitude: } |Y(\omega)| = \{\text{Re}[Y(\omega)]^2 + \text{Im}[Y(\omega)]^2\}^{1/2} \quad \text{A-1.9}$$

$$\text{phase: } \varphi = \tan^{-1} \left\{ \frac{\text{Im}[Y(\omega)]}{\text{Re}[Y(\omega)]} \right\} \quad \text{A-1.10}$$

$$Y(\omega) = |Y(\omega)|e^{j\varphi(\omega)} \quad \text{A-1.11}$$

Where the $\text{Re}[g(\omega)]$ and $\text{Im}[g(\omega)]$ notation signify the real and imaginary components of the function, $g(\omega)$, respectively. The imaginary number $(-1)^{1/2}$ is designated by the variable j .

Electrical power can be characterized in terms of the admittance. First, power is defined in terms of the voltage and current through the relationship:

$$p = \frac{dw}{dt} = \frac{dw}{dq} \frac{dq}{dt} = v(t)i(t) \quad \text{A-1.12}$$

The power in the frequency domain is defined as:

$$P(\omega) = V(\omega)I(\omega) \quad \text{A-1.13}$$

Applying the definition of admittance in Equation (A-1.7), the power characteristics can be defined in terms of the admittance and the voltage.

$$P(\omega) = Y(\omega)V^2(\omega) \quad \text{A-1.14}$$

A-1.1c Discussion of Power (Reference 27)

A few solutions can be developed from the previous definition of power, Equation A-1.14. By breaking down the exponential function into the sine and cosine parts, the power can be expressed by its real and imaginary components:

$$P(\omega) = |Y(\omega)|V^2(\omega)\{\cos(\varphi(\omega)) + j \sin(\varphi(\omega))\} \quad \text{A-1.15}$$

$$\text{Re}[P(\omega)] = |Y(\omega)|V^2(\omega)\cos(\varphi(\omega)) \quad \text{A-1.16}$$

$$\text{Im}[P(\omega)] = |Y(\omega)|V^2(\omega)\sin(\varphi(\omega)) \quad \text{A-1.17}$$

The real component of power is commonly referred to as the "dissipative" power. Dissipative power consumption is generally due to a resistive load in the circuit. This energy loss is dissipated in the form of heat, thus, the power loss is referred to as dissipative power. The imaginary component is commonly referred to as "reactive" power. Theoretically, the reactive component of power does not consume power.

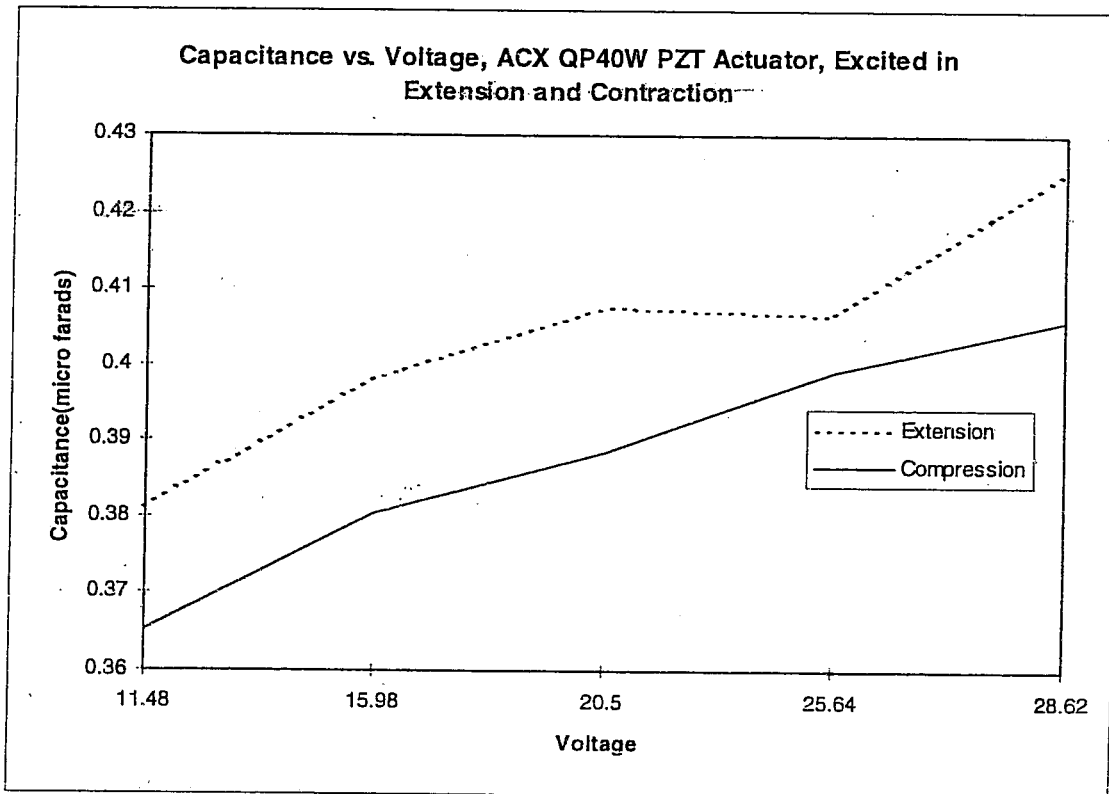
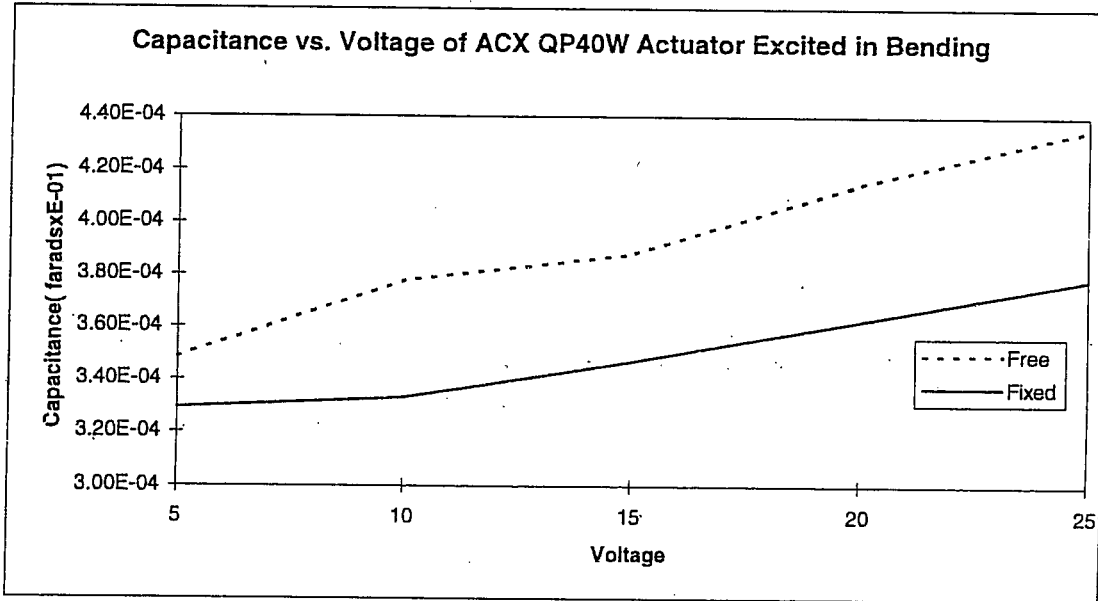
Reactive power is analogous to a mass-spring system in motion. The power will continue to cycle until dissipated by a resistive element, or a damper in the mass-spring system.

Realistically, the power requirements of an electrical system are characterized by the apparent power, or the total magnitude of the power.

$$P_{\text{apparent}}(\omega) = |Y(\omega)|V^2(\omega) \quad \text{A-1.18}$$

Typically, amplifiers that supply the power to a circuit are not capable of storing the reactive power. The reactive power is required to be "replenished" after every cycle. For this reason, the power requirements of a circuit are defined by the apparent power. More complex amplifiers are being produced that store the reactive component of the power, therefore, the total power consumption would be characterized by the dissipative power alone. Because of the variability between amplifier types, knowing the type of amplifier is vital to determining the power requirements of the circuit

APPENDIX-2: Non-Linear Capacitance Plots Highlighting Effects of Changing Boundary Conditions.



APPENDIX-3 ACX Actuator Material Properties and Geometry

Contact information:

Active Control Experts, Inc.
215 First Street
Cambridge, MA 021241-1227

Tel: 617-577-0700

Fax: 617-577-0656

e-mail: info@acx.com

WWW: www.acx.com

Model QP40W Specifications



Application type: strain actuator only

Device size (in): 4.00 x 1.50 x 0.03

Device weight (oz): 0.51

Active elements: 2 stacks of 2 piezos

Piezo wafer size (in): 1.81 x 1.31 x 0.010

Device capacitance: (μF): 0.40

Full scale voltage range (V): ± 200

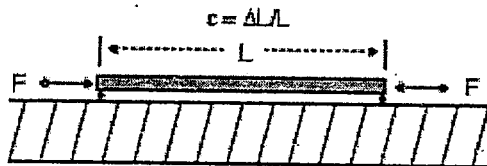
Functional Diagram



Device poled with positive voltage applied to pins 2 and 3.

Bonded Configuration

Full scale strain, extension (μ): ± 280



QuickPack[®] Actuator Piezoelectric Properties			
Property	Symbol	Units	Value
Dielectric Constant (1 KHz)	K_3^T		1800
Dielectric Loss Factor (1 KHz)	$\tan\delta_c$	%	1.8
Curie Point	T_c	°C	350
Density	ρ	kg/m ³	7700
Coercive Field*	E_c	KV/cm	14.9
Coupling Coefficients	K_p		0.63
	K_{33}		0.70
	K_{31}		0.30
	K_i		0.40
Piezoelectric Charge Coefficients (Displacement Coefficient)	d_{33}	$\frac{\text{Coul.}}{\text{Newton}} \times 10^{-12}$	350
	d_{31}	(or) $\frac{\text{meters}}{\text{volt}} \times 10^{-12}$	-179
Piezoelectric Voltage Coefficient (Voltage Coefficient)	g_{33}	$\frac{\text{volt meters}}{\text{Newton}} \times 10^{-3}$	24.2
	g_{31}		-11.0
Elastic Modulus	Y_{11}^E	$\frac{\text{Newton}}{\text{meter}^2} \times 10^{10}$	6.9
	Y_{33}^E		5.5

* Measured at less than 1 Hz.

$$\text{Plate Capacitance (F)} = \frac{K_3^T \epsilon_0 l w}{t}$$

Definitions			
$\tan\delta_c$	- Dielectric Loss Factor	ρ	- Mass Density of Ceramic
T_c	- Curie Point	l	- Length (m)
d_{33}	- Direct Charge Coefficient	w	- Width (m)
d_{31}	- Transverse Charge Coefficient	t	- Thickness (m)
g_{31}	- Transverse Voltage Coefficient	E_c	- Coercive Field
g_{33}	- Direct Voltage Coefficient	ϵ_0	- Permittivity of free space
K_p	- Planar Electromechanical Coupling Coefficient	K_{33}	- Direct Electromechanical Coupling Coefficient
K_{31}	- Transverse Electromechanical Coupling Coefficient	Y_{33}^E	- Direct Youngs Modulus
K_3^T	- Free Dielectric Constant Measured Along Poling Axis	Y_{11}^E	- Elastic Modulus

REFERENCES

1. Rogers, C, Liang, C., *Some Interesting Mechanics Issues for Smart Material Systems*, Proceedings of the International Congress on Experimental Mechanics, 7th Annual, Las Vegas, Nevada, Vol. 1, p. 608-614.
2. Weisshaar, T. A., *Aeroservoelastic Control Concepts with Active Materials*, School of Aeronautics and Astronautics, Purdue University, West Lafayette, Indiana.
3. Kudva, J. N., Appa, K., Martin, C. A., Jardine, A., *Overview of Recent Progress on the DARPA/WL "Smart Materials and Structures Wing" Program*, SPIE's 4th Annual Symposium on Smart Structures and Materials, San Diego, March, 1997.
4. McGowan, A-M.R., Heeg, J., Lake, R.C.: *Results of Wind-Tunnel Testing From the Piezoelectric Aeroelastic Response Investigation*, Proceedings of the 37th AIAA Structural Dynamics and Materials Conference, Salt Lake City, UT, April 1996.
5. Heeg, J., McGowan, A-M.R., Crawley, E., Lin, C.: *The Piezoelectric Aeroelastic Response Tailoring Investigation: Analysis and Open-Loop Testing*, CEAS International Forum on Aeroelasticity and Structural Dynamics, Manchester UK, June 1995.
6. Moses, Robert W.: *Vertical Tail Buffeting Alleviation Using Piezoelectric Actuators and Rudder - Results of the Actively Controlled Response Of Buffet Affected Tails (ACROBAT) Program*, High-Angle -of-Attack Technology Conference, September 17-19, 1996.
7. Pinkerton, J.L., McGowan, A-M.R., Moses, R.W., Scott, R.C., Heeg, J.: *Controlled Aeroelastic Response and Airfoil Shaping Using Adaptive Materials and Integrated*

- Systems*, Proceedings of the 37th AIAA Structural Dynamics and Materials Conference, Salt Lake City, UT, April 1996.
8. Crawley, E. F., de Luis, J., *Use of Piezoelectric Actuators as Elements of Intelligent Structures*, AIAA Journal, Vol. 25, NO. 10, 1987.
 9. Crawley, E. F., Anderson, E. H., *Detailed Models of Piezoceramic Actuation of Beams*, Journal of Intelligent Systems and Structures, Vol. 1-January 1990, pp. 4-25.
 10. Warkentin, D. J., Crawley, E. F., Senturia, S. D., *The Feasibility of Embedded Electronics for Intelligent Structures*, Journal of Intelligent Systems and Structures, Vol. 3-July 1992, pp. 462-482.
 11. Dosch, J. J., Inman, D. J., Garcia, E., *A Self-Sensing Piezoelectric Actuator for Collocated Control*, Journal of Intelligent Systems and Structures, Vol. 3-January 1992, pp. 166-185.
 12. Pan, J., Hansam, C. H., Snyder, S. D., *A study of the Response of a Simply Supported Beam to Excitation by a Piezoelectric Actuator*, Journal of Intelligent Systems and Structures, Vol. 3-January 1992, pp. 3-16.
 13. Song, O., Lirescue, L., Rogers, C. A., *Application of Adaptive Technology to Static Aeroelastic Control of Wing Structures*, AIAA Journal, Vol. 30, No. 12, December 1992, pp. 2882-2889.
 14. Nam, C., Kim, J-S., *Robust Controller Design Of a Wing with Piezoelectric Materials for Flutter Suppression*, The 10th VPI & SU Symposium on Structural Dynamics and Control, May 8-10, 1995, Blacksburg, VA.

15. Akella, P., Chen, X., Hughes, D., Wen, J. T., *Modeling and Control of Smart Structures with Bonded Piezoelectric Sensors and Actuators: A Passivity Approach*, SPIE's 1994 North American Conference on Smart Structures and Materials, Feb. 1994, Orlando, FL, pp. 108-119.
16. Layton, J. B., *An Analysis of Flutter Suppression Using Adaptive Materials Including Power Consumption*, AIAA 1995.
17. Freed, B., Babuska, V., *Finite Element Modeling of Composite Piezoelectric Structures with MSC/NASTRAN*, SPIE's 4th Annual Symposium on Smart Structures and Materials, San Diego, CA, March 1997.
18. Zaglaver, H.W., Last, B., *Modeling Techniques in the Design of Smart Structures for Active Vibration Control*, SPIE's 4th Annual Symposium on Smart Structures and Materials, San Diego, CA, March 1997.
19. Liang, C., Sun, S., Rogers, C.A.: *Dynamic Output Characteristics Of Piezoelectric Actuators*, SPIE's 1993 North American Conference on Smart Structures and Materials, Albuquerque, 1-4 February, 1993.
20. Liang, C., Fanping, S., Rogers, C. A., *Determination of the Optimal Actuator Locations and Configurations Based On Actuator Power Factors*, Proceedings, Fourth International Conference on Adaptive Structures, Cologne, Germany, Nov. 2-4, 1993.
21. Liang, C., Sun, F.P., Rogers, C.A.: *Investigation of the Energy Transfer and Power Consumption of Adaptive Structures*, Proceedings of the 31st Conference on Decision and Control, Tucson, Arizona, December 1992.

22. Zhou, S., Liang, C., Rogers, C.A.: *Coupled Electro-Mechanical Impedance Modeling to Predict Power Requirement and Energy Efficiency of Piezoelectric Actuators Integrated with Plate-Like Structures*, AIAA Paper No. 94-1762, Proceedings of the AIAA/ASME Adaptive Structures Forum, SC, April 1994.
23. Hagood, N. W., Chung, W. H., von Flotow, A., *Modeling Of Piezoelectric Actuator Dynamics For Active Structural Control*, Journal of Intelligent Material Systems and Structures, Vol. 1, No. 3, pp 327-354.
24. Warkentin, David J., Crawley, Edward F., *Power Amplification for Piezoelectric Actuators in Controlled Structures*, MIT Space Engineering Research Center, Cambridge, Massachusetts, SERC #4-95, May, 1995.
25. Sherrit, S., Wiederick, H. D., Mukherjee, B. K., *Field Dependency of Complex Piezoelectric, Dielectric and Elastic Components of Motorola PZT 3203 HD Ceramic*, SPIE's 4th Annual Symposium on Smart Structures and Materials, San Diego, CA, March 1997.
26. Main, J. A., *Charge-Recovery Power Amplifier for Piezoelectric Applications*, SPIE's 4th Annual Symposium on Smart Structures and Materials, San Diego, CA, March 1997.
27. Smith, R.J., Dorf, R.C.: *Circuits Devices and Systems*, 5th Edition, John Wiley and Sons, Inc., 1992.
28. Askeland, D.R.: *The Science and Engineering of Materials*, 2nd Edition, PWS-KENT Publishing Company, 1989.

29. Ashley, S.: *Smart Skis and Other Adaptive Structures*, Mechanical Engineering, Nov.

1995.

